THERMAL EXPANSION AND ISOTHERMAL COMPRESSIBILITY OF SOLID NITROGEN AND METHANE

By
DAVID CRAIG HEBERLEIN

A DISSERTATION PRESENTED TO THE GRADUATE COUNCIL OF
THE UNIVERSITY OF FLORIDA
IN PARTIAL FULFILLMENT OF THE REQUIREMENTS FOR THE
DEGREE OF DOCTOR OF PHILOSOPHY

UNIVERSITY OF FLORIDA
1969

To Martha

ACKNOWLEDGEMENTS

I would like to express my appreciation to the following persons for their contributions towards the completion of this work:

Dr. E. D. Adams, the Chairman of my Supervisory Committee, who assisted in the design and construction of the apparatus and guided the course of this work;

Dr. T. A. Scott for his helpful suggestions in the study of solid nitrogen;

Dr. J. S. Rosenshein for his helpful suggestions in the study of solid methane;

Dr. J. W. Philp for his help in using the computer to analyze the data taken in these experiments;

Doctors J. R. Gonano, P. N. Henriksen, M. F. Panczyck, R. A. Scribner, and G. C. Straty, who all have rendered valuable assistance to me; and,

Mr. B. McDowell, who provided valuable technical assistance and produced the liquid helium necessary to run the experiments.

I would like to thank my parents, Mr. and Mrs. F. A. Heberlein, for their continued help and encouragement during my undergraduate and graduate study. I also would like to thank my aunt and uncle, Dr. and Mrs. R. L. Fairing, for their help and encouragement during my graduate study.

I am grateful to my wife, Martha, for her understanding and encouragement during a long, and,at times, frustrating, graduate study.

TABLE OF CONTENTS

LIST OF FIGURES

Figure Page

I. INTRODUCTION

Nitrogen

Solid nitrogen exists in three distinct phases. The phase diagram as determined by Swenson[1] is shown in Fig. 1. The gamma phase found by Swenson in 1959 exists at low temperatures and high pressures. Very little about the gamma phase is known.

From its triple point to 35.6 K, nitrogen in its beta phase consists of diatomic molecules arranged in a hexagonal-close-packed lattice. The space group $P6_3/mmc$ was determined from x-ray studies by Boltz et al.[2] in 1959. Molecular rotation in the beta phase was confirmed from x-ray studies by Jordan et al.[3] and Streib et al.[4] and from studies of the infrared spectrum by Smith et al.[5] The quenching of the quadrupole coupling in beta nitrogen can only be explained by either spherical rotation as found in liquid nitrogen or by hindered rotation with the molecular axis inclined at an angle of 54.7°. Because the specific heat is found to have a value 50% greater than that needed for free rotation and the molecular volume is only 75% of that expected for freely rotating molecules, the rotations are not free. Thus, there is a hindered rotation in which the molecular axis makes an angle of 54.7° with the crystal axis.

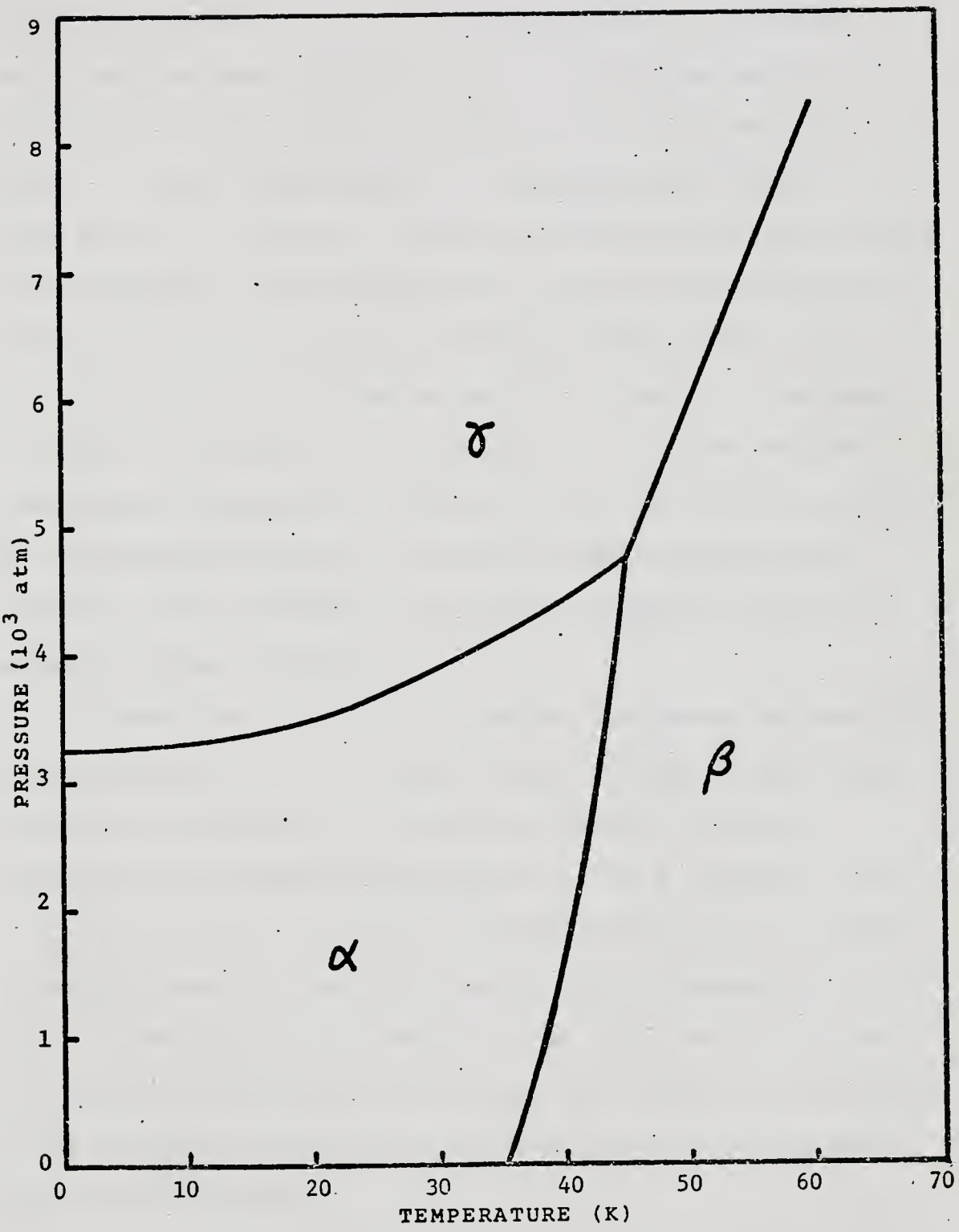

Fig. 1. Phase diagram of solid nitrogen. Pressure versus temperature.

At 35.6 K, solid nitrogen at its vapor pressure undergoes a first-order phase transition with a latent heat of 54.7 cal/gm-mole.[6,7] The lower temperature, alpha phase has a face-centered-cubic lattice in which the centers of each molecule are displaced slightly from the lattice points. X-ray measurements by Jordan et al.[3] showed the space group to be $P2_13$. Because alpha nitrogen has a rather open structure, it is reasonable to assume that the nuclear quadrupole coupling constant, e^2qQ/h, differs very little from its value in the free molecule. Using pure quadrupole resonance continuous wave techniques, Scott[8] determined the temperature dependence of e^2qQ/h. The result of this study and subsequent studies by DeReggi[9] found the resonance frequency to be extremely temperature dependent near the alpha-beta phase transition.

Although most theories of solids are given for constant volume processes, it is easier experimentally in most cases to make measurements at constant pressure. In order to distinguish the temperature dependence of a quantity such as the quadrupole resonance frequency, which is measured at constant pressure, from that caused by the expansion of the lattice, the equation of state of the solid must be known. To determine the equation of state, the temperature dependence of the expansion coefficient and the isothermal compressibility must be known.

Until recently, little experimental information other than the specific heat was available on the thermal properties

of solid nitrogen. In 1966, Manzhelii, Tolkachev, and Voitovich[10] (MTV) measured the expansion coefficient of solid nitrogen from 22 to 44 K. In an attempt to extend these measurements to 4.2K, the expansion coefficient was measured from 4.2 to 38 K in this work. Recently, Bezuglyi, Tarasenko, and Ivanov[11] (BTI) determined the adiabatic compressibility from 16 to 44 K from their measurements of the velocity of sound in solid nitrogen. The isothermal compressibility, K_T, is simply related to the adiabatic compressibility, K_S, by

$$K_T = K_S + \alpha^2 T v C_p^{-1} \quad , \qquad (1)$$

where α is the expansion coefficient, T the temperature, v the molar volume, and C_p the specific heat at constant pressure. Thus, the isothermal compressibility of solid nitrogen was measured in this work from 8 to 40 K as a consistency check not only on the measurements of BTI, but also as a check on the temperature dependence of the expansion coefficient.

Methane

The existence of a λ anomaly in the specific heat of solid methane at 20.4 K was first observed in 1929 by Clusius.[6] Because the maximum in the specific heat appeared to be finite, the transition was assumed to be of second-order. X-ray diffraction studies by Schallamach[12] showed no change in the face-centered-cubic structure of solid methane at 20.4 K, with the lattice constants differing by approximately 1% on opposite sides of the transition.

This small change in the molecular lattice indicates that the thermal anomaly involves a change in the orientational ordering of the molecules of the lattice.

Pauling[13] originally described the transition as involving a sudden change from molecular oscillations in the low temperature phase to free molecular rotation in the higher temperature phase. This was consistent with the approximate value of 3 cal/mole for the specific heat above the transition. Proton spin resonance experiments by Thomas et al.[14] determined that this picture of the transition was not correct. The resonance line width observed by Thomas et al. indicated no perceptible change at 20.4 K, and only above 65 K did the line width and characteristic time for spin-lattice relaxation both drop toward the values observed in liquid methane. Studies of the Raman bands at 79 K by Crawford[15] showed rotational wings of the same size as those found in liquid methane. Thus, while the hindrance to molecular rotation is small above 65 K, the phase change in solid methane at 20.4 K takes place without the establishment of free molecular rotation. Although the passage to free rotation does occur, it occurs gradually at higher temperatures, and without the appearance of a thermal anomaly.

The phase diagram of solid methane is shown in Fig. 2. There are four solid phases in methane. The alpha phase has been extensively studied and the alpha-beta and alpha-gamma phase boundaries have been determined from the specific heat measurements of methane under hydrostatic pressure by

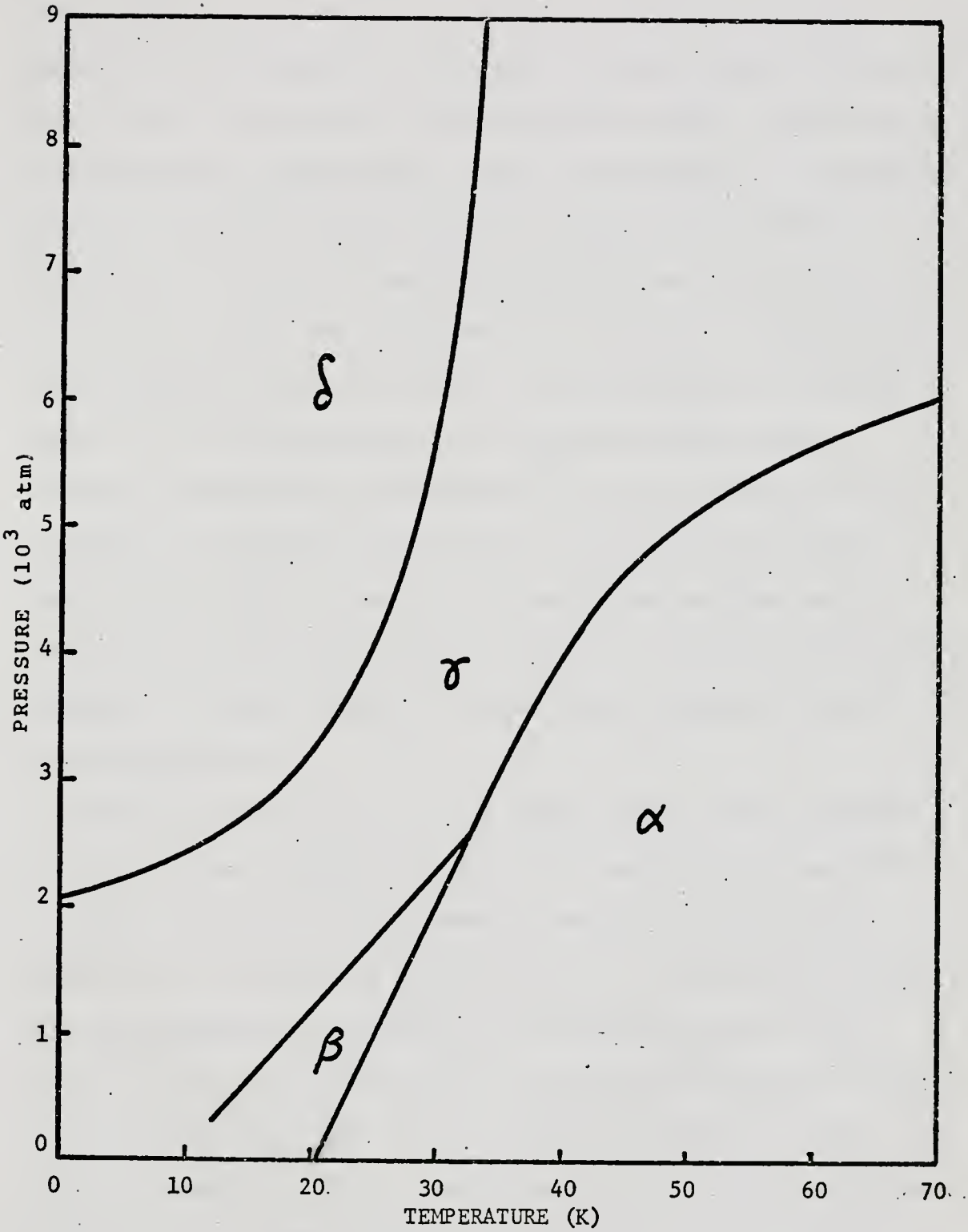

Fig. 2. Phase diagram of solid methane. Pressure versus temperature.

Rosenshein[16] and from the p-v isotherms determined by Stevenson[17] and Stewart.[18] The delta phase was first reported by Stevenson in 1957 and to date nothing more is known about this phase. The beta-gamma phase boundary has been observed to pressures as low as 200 atm. by Rosenshein, or about 800 atm. lower than that observed by either Stevenson or Stewart. Recent specific heat measurements by Colwell, Gill, and Morrison[19] (CGM) show a broad excess heat capacity in solid methane at zero pressure centered about 8 K. An extrapolation of the beta-gamma phase boundary determined by Rosenshein to zero pressure gives a transition temperature of 9.5 K. While the agreement seems reasonable in view of the broadness of the lower temperature transition, there exists no other experimental evidence to extend the beta-gamma phase boundary to 8 K at zero pressure.

With the exception of the early molar volume studies of solid methane between 20 and 21 K reported by Heuse[20] in 1936, virtually no information exists on the thermal expansion of methane at or below 21 K. In this work, the thermal expansion of methane was measured from 4.2 to 26 K not only to determine the lattice contribution to the thermal expansion, but also to study the nature of the thermal anomaly at 20.4 K and to determine if possible the existence of a lower temperature phase at zero pressure.

II. THEORY

In 1936 Pauling[13] suggested that the transitions in solid CH_4, N_2, O_2, and CO_2 were caused by a change from oscillation to free rotation of the molecules. He approximated the effect of the crystal field on the molecule with the potential

$$V(\theta) = V_o(1 - \cos 2\theta) \qquad (2)$$

in which θ is the angle between a molecular axis and its equilibrium position. This form is, however, a poor representation of the dipole interaction which depends not only on the relative orientation of the two dipoles, but also on the direction of the vector separating their centers. Furthermore, it has been shown by Kirkwood[21] that a potential of this form always leads to a prediction of a single second-order transition.

Kreiger and James[22] showed that the interaction potential

$$V = A\cos\theta_{ij} + B\cos^2\theta_{ij} \qquad (3)$$

could lead to a single second-order transition, a single first-order transition, two first-order transitions or a second-order transition followed by a first-order transition for increasing temperature. Both of these models are much oversimplified in that they assume axial symmetry of the molecules and they treat the interaction of the molecules as dependent only on the orientations of the molecules in

space irrespective of the position of each molecule in the lattice.

Nitrogen

Kohin[23] found the directional interaction potential for solid nitrogen to be

$$V(\theta) = CIP_2(\cos\theta) \quad , \qquad (4)$$

where I is the average of $P_2(\cos\theta_i)$ for the neighbors of a central molecule, θ the angle that each molecule makes between the molecular axis and the symmetry axis at its lattice site, $P_2(\cos\theta) = -(1/2) + (3/2)\cos^2\theta$, and C a function of the lattice constants and molecular parameters as determined from nearest and next-nearest neighbor interactions. Eq. (4) is a combination of the following terms: a term due to the interaction of the quadrupole moments of the molecules; a directional correction to the attractive dispersion forces due to the anisotropic polarizabilities of the molecules; and, a directional correction to the repulsive forces.

If an assembly of classical rigid rotors with fixed centers is taken as a model for a crystal of diatomic molecules, the normalized rotational distribution function is

$$f(\theta,\phi) = \frac{\exp(-V(\theta,\phi)/kT}{\int \exp(-V(\theta,\phi)/kT dw} \quad , \qquad (5)$$

where $f(\theta,\phi)dw$ is the probability that the axis of the molecule lies in the solid angle dw about (θ,ϕ). $V(\theta,\phi)$ is the orientational potential due to the crystal field. If one now assumes that each molecule orients itself independently in

the average field of its neighbors and that the probability distribution for molecular orientation is the same for each lattice site, we can then require the rotational distribution to be consistent with the crystal field to obtain a consistency equation relating the temperature and the order parameter. Since I has been defined as the assembly average of $P_2(\cos\theta)$, the classical consistency relation for I(T) becomes

$$I(T) = \frac{\int P_2(\theta)\exp(-CIP_2(\theta)/kT)dw}{\int \exp(-CIP_2(\theta)/kT)dw} . \qquad (6)$$

There are two solutions to Eq. (6). One solution corresponds to rotational disorder, i.e. $V(\theta,\phi) = 0$ for all temperatures. The other solution, corresponding to an ordered array, has an extremum corresponding to a maximum in the temperature. The calculated T_{max} then corresponds to a theoretical upper bound on the alpha-beta transition. Using a classical model similar to this, Jansen and de Wette[24] obtained a value for T_{max} very close to 35.6 K. Kohin pointed out, however, that when the directional anisotropy of the intermolecular repulsive forces are included as in Eq. (6), the calculated transition temperature becomes much higher.

By treating the diatomic nitrogen molecule as a rigid rotor, Kohin solved the Schrödinger equation to find the eigenvalues for the directional potential given in Eq. (4). By minimizing the directional energy of the crystal field, the acceptable orientations of the molecules agree with the observed structure for alpha nitrogen. Since the method used by Kohin assumes that the molecules are stationary and consequently near absolute zero, no attempt was made to

determine theoretically the structure for beta nitrogen. Furthermore, it would be erroneous to attempt to extend this theory to temperatures higher than 20 K without including such effects as the lattice vibrations and direct correlations between neighbors. Since there exists no microscopic theory to explain the behavior of alpha nitrogen above 20 K, we must turn to some phenomenological approaches based on experimental observations.

DeReggi, Canepa, and Scott[25] found that the pure quadrupole resonance frequency, ν_Q, obeys an order parameter relation of the form

$$\nu_Q = A\left[\frac{(T_c - T)}{T_c}\right]^{\beta}, \qquad (7)$$

such that

$$\left[\frac{1}{\nu_Q}\frac{d\nu_Q}{dT}\right]^{-1} = -\frac{1}{\beta}(T_c - T) \ . \qquad (8)$$

By plotting $-\nu_Q(\partial\nu_Q/\partial T)^{-1}$ versus temperature, these authors found that their experimental points gave a straight line from approximately 20 K to the transition temperature. Extrapolating this line to its intersection with the temperature axis gave a critical temperature $T_c = 37.70 \pm 0.07$ K. From this behavior it appears that there exists a higher order process in alpha nitrogen. The process is interrupted before completion by the first-order transition. A similar behavior is found in solid hydrogen[26] in which a change in crystal structure interrupts the progress of a higher order process.

A phenomenological approach to explain the large rise in heat capacity and the thermal expansion from 20 K to the transition at 35.6 K has been proffered by MTV.[10] A number of solids behave in a similar manner as the melting point is neared. The changes in the thermal properties other than that which can be ascribed to the nominal expansion of the lattice are explained by a rapid growth in the number of vacancies. In analogy to the rapid growth in the number of vacancies, MTV suggested that as the temperature rises there is a rapid growth in the number of disoriented molecules in alpha nitrogen until the lattice becomes unstable. At this temperature a phase transition occurs, and a different crystal structure appears.

To explain the formation of these "orientational defects", the free energy of the crystal would have to decrease. In order for the free energy to decrease, the gain in potential energy due to the new orientation about which the molecule oscillates has to be exceeded by a gain in entropy from the decrease in orientational order.

If it is assumed that the production of disoriented molecules is accompanied by an increase in volume, then the change in volume may be expressed as

$$\Delta v = Kc \ , \qquad (9)$$

where K is a constant of proportionality and c is the concentration of orientational defects. The concentration of these orientational defects should obey an exponential law of the form

$$c = A\exp(-U/RT) \ , \qquad (10)$$

where A is a degeneracy factor equal to the number of positions of disoriented molecules having the same energy, U the activation energy to create the orientational defect, R the natural gas constant, and T the temperature. Combining Eq. (9) and Eq. (10), we find the relative change in length, dl/l, to be given by

$$\frac{\Delta l}{l} = \frac{\Delta v}{3v} = \frac{KA}{3v}\exp(-U/RT) \ , \qquad (11)$$

or

$$\ln(\Delta l/l) = \ln(KA/3v) - U/RT. \qquad (12)$$

By assuming that at some temperature, T_1, the influence of the orientational defects is negligibly small and that the coefficient of thermal expansion connected with other mechanisms remains well-behaved as the temperature is raised above T_1, then any major portion of the plot of $\ln(\Delta l/l)$ versus $1/T$ that gives a straight line can be said to obey the predicted exponential behavior. From their thermal expansion data, MTV found this behavior in the interval 29.4-34.5 K using a T_1 = 23 K. From the slope of this line, MTV calculated an activation energy of 450 cal/mole. The difficulty with this approach is that both the slope of $\ln(\Delta l/l)$ versus $1/T$ and the interval for which a straight line pertains depends on the choice of T_1. Ideally, Δl would approach zero as T approaches 0 K, but in reality the exponential behavior is only observed for temperatures above 20 K. This approach is useful because it is possible to determine in approximately which temperature interval a mechanism with an exponential temperature dependence begins to dominate the thermal expansion.

A similar approach by Bagatskii, Kucheryavy, Manzhelii, and Popov[27] (BKMP) to explain the excess heat capacity above 20 K gave an activation energy of 460 cal/mole. In view of the approximations made by BKMP for the lattice contribution to the specific heat and the inherent error in the determination of the activation energy by MTV, the agreement appears fortuitous. The phenomenological approach of MTV is of interest, however, because there appears to be nothing in the potential found by Kohin to explain the strong temperature dependence of the expansion coefficient, the isothermal compressibility, the excess heat capacity, or the pure quadrupole resonance frequency at temperatures above 20 K.

Methane

Fortunately, methane with its high molecular symmetry and relatively large intermolecular spacing is a favorable case for studying orientational coupling. In methane the ratio of the intramolecular distance to the molecular separation is so small that one can expect the octopole-octopole interaction between next neighbors to be dominant. Keenan and James[28] have shown for methane that the electrostatic interaction for non-overlapping molecules falls off as rapidly as R^{-7} and by neglecting all interactions except those between nearest neighbors in a crystal, they were able to formulate a theory for solid methane in terms of a single adjustable parameter, the effective octopole moment of the molecule.

In the model developed by Keenan and James, molecular and lattice vibrations are neglected and the methane crystal was treated as a face-centered-cubic array of spherical rotors carrying a charge distribution with tetrahedral symmetry. The statistical calculation is a classical version of the self-consistent field approach in which the conditions for self-consistency appear as a family of integro-functional equations, one for each molecule in the crystal. Neglect of quantum effects makes the results applicable only to CD_4. Three solutions of these equations minimize the free energy in a particular temperature range. At the lowest temperatures the stable phase has a tetragonal symmetry with the molecules oscillating about equivalent equilibrium orientations. As the temperature rises, the crystal undergoes a first-order transition into a phase with octahedral symmetry in which one molecule in four rotates freely. As the temperature rises even higher the crystal undergoes a second-order transformation to an orientationally disordered phase. By assigning a value to the molecular octopole moment to make the higher transition temperature agree with the 27.4 K value observed in CD_4, the predicted lower transition temperature becomes 24.4 K as opposed to the observed temperature of 22.2 K. The predictions of this theory are in agreement with integrated heats of transition, zero-point entropy and the optical properties of all three phases.

An extension of this model to include solid CH_4 has recently been completed by Yamamoto and Kataoka.[29] The high and low temperature ordered phases are assumed to have the same sub-lattice structure as that proposed by James and Keenan, but differ in that all calculations were made on the basis of quantum statistical mechanics in the subspace $J \leqq 4$, where J is the rotational quantum number. Since the various spin combinations of the hydrogens produce three separate spin species, A (meta), E (para), and T (ortho), the nuclear spin species are treated separately. Inasmuch as the high temperature equilibrium proportions of A:E:T become frozen in at low temperatures, the results for individual spin species can not be compared in any other than a qualitative way with experimental measurements on samples with "mixed" spin species. The most interesting feature of this quantum mechanical treatment of solid methane is the prediction that for a sample of spin species A, two phase transitions, one at 20.7 K and the other at 16 K, are to be expected. This is to be compared with the specific heat measurements on "mixed" crystals by CGM, whose results showed transitions at 20.4 K and 8 K.

Thermodynamically the large specific heat anomaly in methane has been described as a cooperative transition. To describe what is meant by a cooperative transition, let us assume for the moment that methane obeys a van der Waals equation of state

$$(P + av^{-2})(v - b) = RT \ , \qquad (13)$$

in which the term av^{-2} is a correction to the pressure to allow for the attractions of the molecules, and b is a term to allow for the fact that the molecules are of a finite size. The term av^{-2} increases in importance as the volume decreases, such that if the temperature is steadily reduced it becomes thermodynamically advantageous for the entire lattice to change abruptly in volume. The loss in entropy from this change would be offset by the gain in energy from the work done by the attractive forces. Thus the presence of a term such as av^{-2} becomes increasingly important with the progress of the change which it is causing, and it is in this sense that the transition was called cooperative by Fowler.[30,31] Furthermore, the presence of av^{-2} also points out that a transition of this type can only be understood if some account of the molecular interactions is included in the theory of solids displaying this type of behavior.

The dominant interaction in solid methane has been shown to be the octopole-octopole interaction which lead to a type of orientational ordering of the methane molecules below 20.4 K. Before ordering can occur, the energy in excess of that allowed for the new molecular orientation must first be dissipated in the lattice. Consequently, there appears a large change in the specific heat. The term cooperative is applied to the specific heat anomaly in methane because the transition is very broad.

III. APPARATUS AND PROCEDURE

In this section the design and construction of the apparatus necessary to measure thermal expansion and isothermal compressibility of heavy solidified gases will be presented. A capacitance technique will be described for measuring changes in the length of the sample corresponding to changes in temperature or pressure.

The cryogenic considerations including appropriate plumbing and electrical connections will be considered in a section devoted to the cryostat. The attainment of temperatures ranging from 4.2 to 90 K is discussed in this section with particular emphasis on the control and measurement of temperatures in the interval 52-77 K.

The sample gas handling and helium pressure systems are discussed in the second section of this chapter. Particular emphasis is placed on the purification of the samples used and on the means of controlling the pressure transmitted to the samples.

The third section of this chapter describes the sample chamber and the pressure bomb. The design of the sample chamber is dictated by the thermal properties of the samples which were studied. The concomitant problems of the design necessary for filling the sample chamber at temperatures from 63 to 90 K and of making sample measurements from

4.2 to 40 K are discussed. The construction of a pressure bomb which contained the fluid helium used to transmit hydrostatic pressure to the sample is also presented in this section.

A germanium resistance-thermometer was used to monitor the temperature of the sample. The associated electronics and plumbing used in measuring, calibrating, and regulating temperatures in the interval 4.2-40 K are discussed in the fourth section of this chapter.

The final section in this chapter describes the experimental procedure used to form the sample and to make measurements of the thermal properties of each sample.

Cryostat

The cryostat used to perform these experiments is similar to that described by Walsh[32] and is shown schematically in Fig. 3. The sample chamber and pressure bomb were surrounded by two exchange chambers which in turn were enclosed by two large stainless steel dewars. The outer dewar was usually filled with liquid nitrogen. The required sample temperatures determined the refrigerant to be used in the inner dewar. Thus, liquid nitrogen was used as a refrigerant to obtain temperatures from 52 to 90 K and liquid helium was used as a refrigerant to attain temperatures from 4.2 to 52 K. The refrigerant contained in the inner dewar will be referred to hereafter as the main bath.

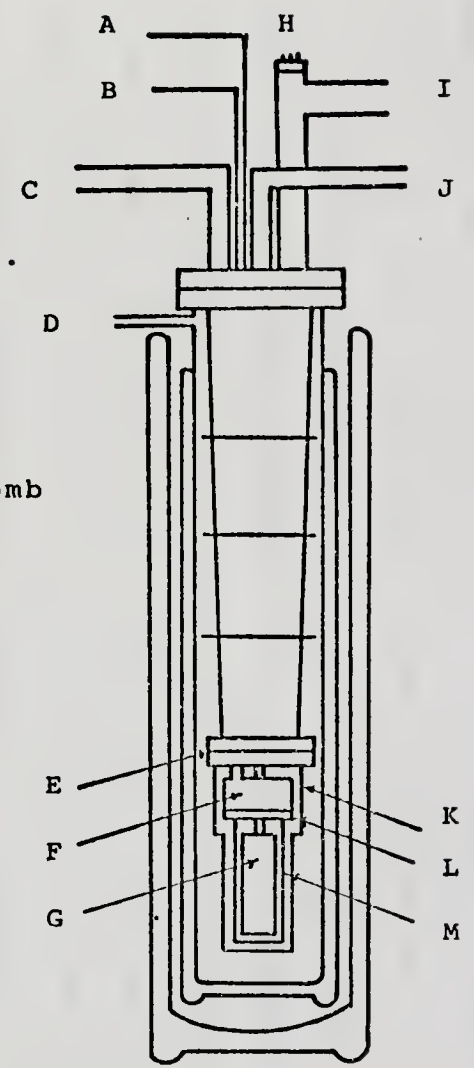

Fig. 3. Schematic drawing of apparatus.

A. Sample filling capillary
B. He^4 pressure capillary
C. Inner bath pumping line
D. He^4 recovery line
E. Outer exchange sealing flange
F. Inner bath
G. Sample chamber and pressure bomb
H. Electrical leads
I. Outer exchange pumping line
J. Inner exchange pumping line
K. Outer exchange vacuum jacket
L. Inner exchange sealing flange
M. Inner exchange vacuum jacket

The outer exchange chamber consisted of a vacuum jacket connected to the stem of the cryostat with a flange-type seal using an indium gasket. The outer exchange chamber was used to isolate the sample chamber from the main bath.

A cylindrical container was enclosed by the outer vacuum jacket. This container had a volume of approximately 250 cm^3 and could be filled with liquid from the main bath by means of a modified "Hoke" valve. The liquid in this container will be referred to hereafter as the inner bath.

A smaller vacuum jacket connected to the base of the inner bath container with another flange-type seal formed the inner exchange chamber. The inner chamber was used to either isolate the sample from the inner bath, or, when filled with exchange gas, to provide thermal contact between the sample and the inner bath.

To form the solid samples, the entire sample system was first cooled to 77 K by filling the main bath with liquid nitrogen. The inner bath container was then filled with liquid nitrogen and the temperature of the sample was controlled by reducing the vapor pressure of the nitrogen. Temperatures from 52 to 77 K could be maintained by pumping the nitrogen with a model KC-46 Kinney pump. The sample chamber and the inner bath had to be maintained at a temperature below the triple point of the sample in order to form a crystal. Therefore, to fill the sample chamber, the sample within the filling capillary had to be heated above its melting point. A 0.0225" O.D. stainless steel

capillary was run through a 0.25" O.D. stainless steel tube which extended to the top of the cryostat. The filling capillary was electrically grounded only at the top of the sample chamber and was thermally isolated from the main and inner baths, permitting the temperature of the entire length of capillary to be raised by connecting a 6-volt storage battery between the capillary and the cryostat ground. The capillary to the pressure bomb was connected in a similar manner such that, if it became blocked by frozen impurities, moderate heating would establish pressure transmission over the entire length of the capillary.

After forming the sample, the liquid nitrogen was removed from the inner dewar. The sample was then cooled to 4.2 K by transferring liquid helium into the inner dewar. Two separate heating coils were wound on the outside of the inner vacuum jacket. Using these heaters, the entire inner chamber could be maintained at temperatures much above that of the main bath. The larger heating coil had a total resistance of 5000-ohms, and, when used with a Heathkit Model PS-4 Regulated Power Supply, provided a course temperature control from 4.2 to 52 K. The smaller coil had a total resistance of 1000-ohms and was used as a fine control on the temperature.

Individual 0.059" O.D. stainless steel capillaries run through separate 0.25 O.D. stainless steel tubes

which extended from the outer vacuum jacket flange to the top of the cryostat formed coaxial lines which were used for capacitance leads. The leads to the heaters and auxiliary thermometers were introduced through the pumping tube into the outer exchange chamber. These leads were made from #36 Advance wire and were thermally anchored to the inner bath container. Vacuum-tight glass-to-metal seals were used to bring electrical leads through the inner bath container into the inner vacuum chamber. The leads into the inner exchange chamber for the germanium resistance-thermometer consisted of two separate 0.059" O.D. stainless steel capillaries introduced through the pumping tube. A 4" section of #36 Advance wire was attached to both of these stainless steel leads before thermally anchoring them to the sample chamber.

Gas Handling and Pressure System

Purification of gas samples was necessary before introduction into the sample and pressure systems. Because impurities such as oxygen and nitrogen in methane could pass through a cold trap held at a temperature near the triple point of methane, a special process was used to purify the methane samples.

C.P. Grade methane, 99.0% pure, was transferred into a one liter cylinder and then immersed in liquid nitrogen. This quick freezing of the methane produced a shattered solid with a large surface area. Since the major

contaminants had a vapor pressure much higher than that of methane at 77 K, the residual vapors could be pumped away until the pressure over the solid was that appropriate to the pure substance. This process was repeated until the newly formed solid had the correct vapor pressure.

C.P. Grade nitrogen, 99.7% pure, was purified by passing the gas sample through a liquid nitrogen cold trap before it entered the U-tube. Similarly, the helium gas used to pressurize the bomb was passed through a helium cold trap before reaching the U-tube.

The gas handling system, shown schematically in Fig. 4, consists of a sample line and a pressure line, both interconnected to a mercury U-tube pressure system. The pressure system was of standard U-tube design and has been adequately described by Straty.[33]

In operation the sample was admitted into the U-tube and subsequently into the filling capillary. The pressure of the gas in the U-tube was then raised, creating a pressure difference between the sample cell and the U-tube. This pressure head produced rapid condensation of the gas into the sample chamber. After forming the sample, the valve between the filling capillary and the U-tube was closed and the gas remaining in the U-tube was pumped away.

In order to measure the isothermal compressibilities of samples, helium gas from a helium cylinder with a high pressure regulator was then introduced into the U-tube and the pressure capillary. Since the volume of the U-tube was

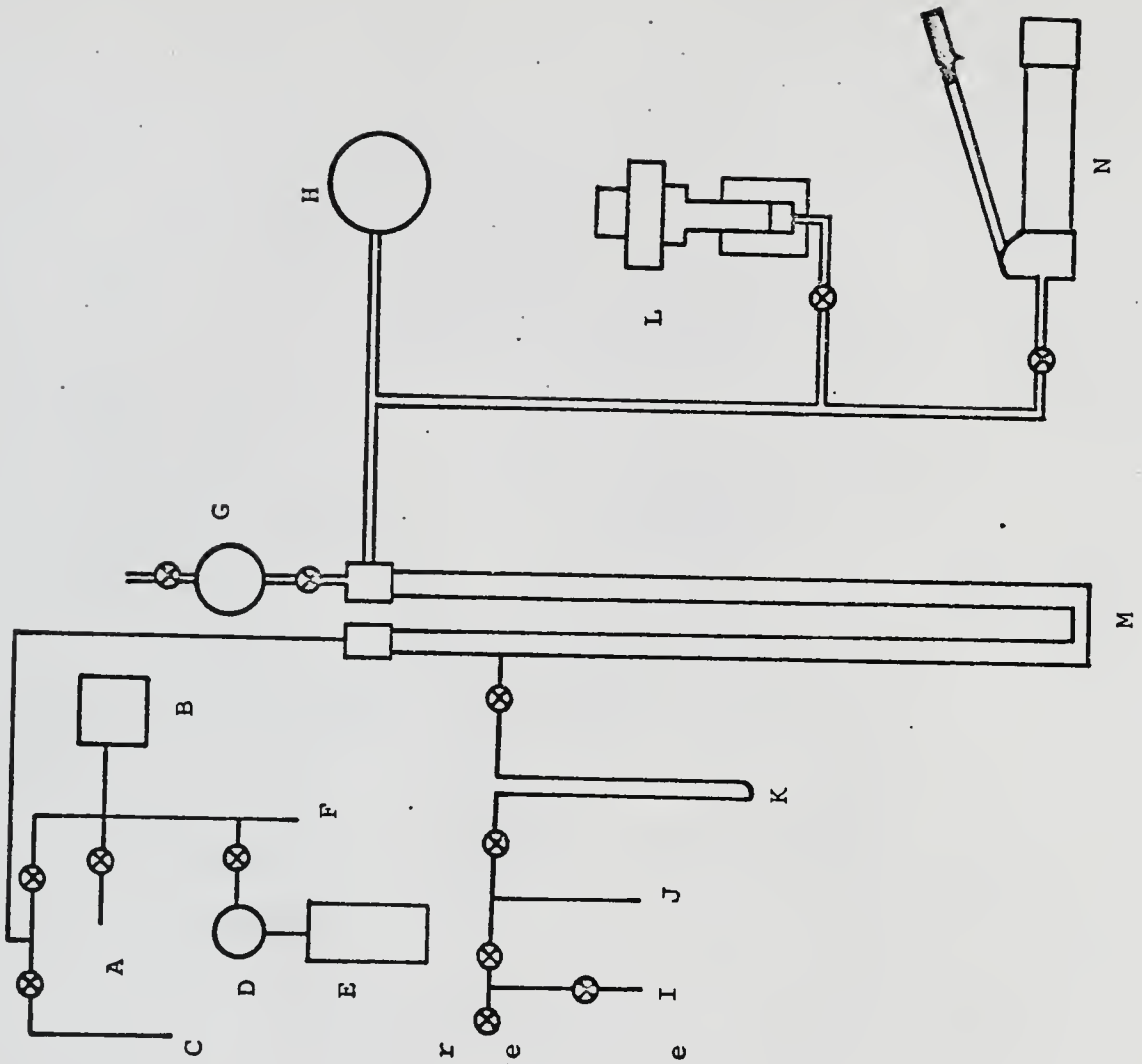

Fig. 4. Pressure system
A. Pressure relief port
B. Texas Instruments gauge
C. Sample capillary
D. High pressure regulator
E. He^4 high pressure cylinder
F. Pressure capillary
G. Oil reservoir and air purge
H. Pressure gauge
I. Sample storage
J. Vacuum line
K. Nitrogen cold trap
L. Free piston pressure gauge
M. U-tube
N. Hydraulic pump

approximately twenty times the dead volume of the pressure bomb, the height of the mercury on the gas side of the U-tube was used to vary the pressure of the gas trapped in the bomb. To prevent mercury from entering the hydraulic lines, a high-level alarm was installed on the oil side of the U-tube. Because the entire U-tube assembly was electrically insulated from its supporting structure, the mercury itself was used as a switching device to actuate the alarm.

A Texas Instruments pressure gauge was connected through appropriate valving into the gas side of the U-tube and was calibrated against a dead weight gauge connected into the oil side of the U-tube. Special care was taken to insure that the mercury levels in the U-tube were equal when calibrating the Texas Instruments pressure gauge reading against the dead weight gauge pressure.

Sample Chamber and Pressure Bomb

Two different approaches were available for measuring thermal expansion and compressibility in solid nitrogen and methane. One approach, which has been used successfully in studies of solid helium,[34] was to measure $P = P(T)$ for fixed molar volumes. The second approach was to measure $V = V(T)$ for fixed pressures.

When solid is formed in a sample chamber, the solid also plugs the filling tube, isolating the chamber from external pressure sensing devices. As the solid is cooled

below its melting point, the internal pressure also decreases. Assuming a Debye solid, this change in pressure can be expressed as

$$\Delta p = \int C_v v^{-1} dT = \gamma \theta_D v^{-1} \int C_v d(T/\theta_D) , \qquad (14)$$

where γ is the Gruneisen parameter, v the molar volume, and θ_D the Debye temperature. Between 90 K, the melting point of methane, and 4.2 K, the change in the internal pressure of methane would be approximately 10^3 atm. It therefore seemed unreasonable to attempt to design a chamber capable of withstanding 10^3 atm. at 90 K and yet retaining sufficient sensitivity to measure changes of less than 1 atm. at 4.2 K.

Fortunately, the heavier solidified gases have a coefficient of thermal expansion on the order of $10^{-4} K^{-1}$ over most of the temperature interval below their melting points. It was more reasonable to design a chamber whose volume would be determined by the solid sample which it surrounded.

Since the crystalline fields in both solid methane and nitrogen are isotropic,[29] it was possible to consider geometries for the sample chamber in which only length changes would be observed. By choosing a chamber with cylindrical geometry, one end of the chamber could be fixed, and the active end would then be used as the moving plate of a three-terminal capacitor. Relative changes in length would be directly related to changes in capacitance as monitored by a General Radio type 1620-A capacitance

measuring assembly. A brass bellows with a small Hooke's law constant was chosen as the sample chamber, both for its radial strength and for its ability to distend elastically over 20% of its equilibrium length.

In making measurements of changes in length, it was necessary to have the bellows distended from its equilibrium position by the solid which it surrounded. Since the solid contracted uniformly as it was cooled, any solid caught in the convolutions of the bellows would contract at the same rate as the total length of the sample.

The change in volume upon melting in both methane and nitrogen is approximately 10% of the total liquid volume. To maximize the capacitive sensitivity, the distance between the moving and the fixed plate, referred to as the gap length (l_g), must be minimal. To minimize the gap length in spite of the large volume change upon melting, two further considerations were incorporated in the design of the sample chamber.

The easiest means of filling the bellows with solid was to sublimate the gas coming through the filling capillary directly into the sample chamber. For sublimation to occur, a thermal gradient along the length of the sample chamber had to be maintained. Since the filling capillary would necessarily have to be at or above the melting temperature of the sample gas, the heated capillary was introduced through the less massive, copper plug at the active end of the bellows. The more massive, supporting

structure for the fixed end of the bellows was thermally anchored to the inner bath. The sample formed in this manner was not homogeneous.

Once the bellows was filled with solid, it was desirable to form as homogeneous a sample as possible. To form a good crystal meant that the material trapped in the bellows would have to be melted and frozen again very slowly. To allow for this large excursion in length, the active end of the bellows was allowed to push a spring loaded, "fixed" capacitor plate away from the stops in its supporting structure. As the liquid began to solidify, the active end of the bellows returned slowly to a position such that the fixed plate was again pushed against the stops in its supporting structure, and the two plates were no longer shorted to one another.

To apply hydrostatic pressure directly to the sample, the area both inside and outside the bellows had to be filled with fluid helium. To surround the sample with fluid helium, a pressure capillary was introduced through the copper support assembly into the sample area. To contain the pressurizing fluid outside the bellows, the entire sample chamber was enclosed inside a pressure bomb.

The sample chamber, surrounded by the pressure bomb, is shown in Fig. 5. Copper was used extensively throughout the sample chamber for two reasons. Copper has a high thermal conductivity, insuring reasonable thermal

Fig. 5. Sample chamber and pressure bomb

A. Pressure bomb
B. Spring
C. Fixed capacitor plate
D. Stops
E. Active capacitor plate
F. Filling capillary
G. Bellows sample chamber
H. Large hollow copper cylinder
I. Detachable copper piece
J. Copper support assembly
K. Copper gasket
L. Pressure plug
M. Stainless steel thermal standoff
N. Thermometer mounting assembly
O. Thermometers
P. Copper cage assembly
Q. Small hollow copper cylinder
R. Pressure capillaries

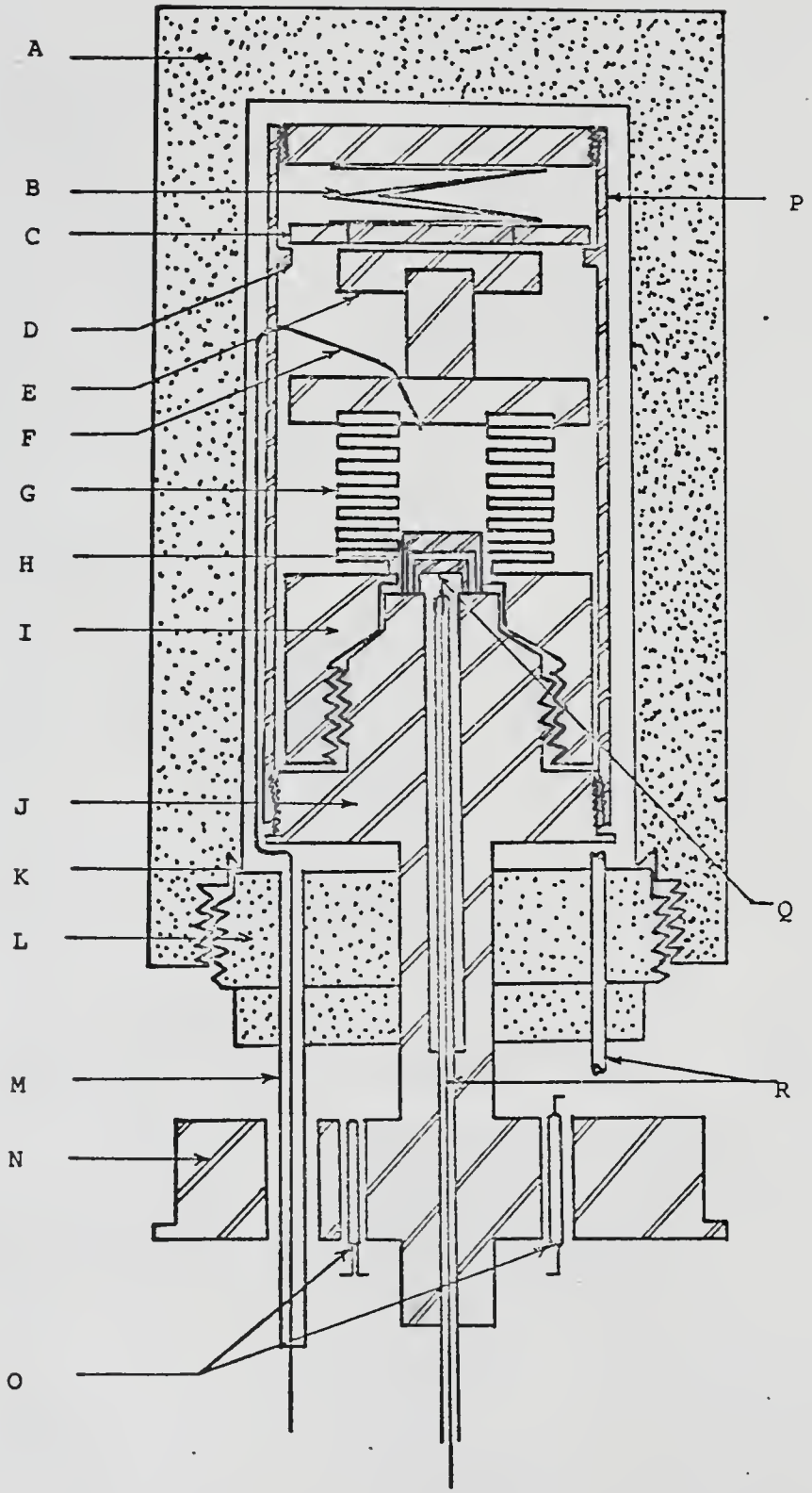
A
B
C
D
E
F
G
H
I
J
K
L
M
N
O
P
Q
R

equilibrium times. Also the thermal expansion of copper is not only small below 77 K, but is also well known.

The sample chamber consisted of a brass bellows, approximately 0.50" in length, with an I.D. of 0.350" and an O.D. of 0.592". The active end of the bellows was soldered to a copper plug. A cylindrical capacitor plate with a diameter of 0.500" was fastened with epoxy to the opposite end of the copper plug. The epoxy electrically insulated the capacitor plate from ground.

The fixed end of the bellows was soldered into a detachable copper piece. At the opposite end of this piece a hub was tapped to receive a plug extending from the copper supporting structure. The plug, when covered with 0.001" Teflon tape, seated on a 45° surface in the bottom of the hub, thus served as the pressure seal to the chamber. To insure that the solid was exposed only to an active portion of the bellows, a hollow copper cylinder, closed only at its top, was mounted on top of the threaded copper plug. The diameter of the cylinder was 0.350" to insure a mechanically tight, but not gas tight, seal to the inside of the bellows. The length of the cylinder was 0.200", implying that the closed end of the cylinder protruded 0.072" into the active portion of the bellows.

Inside the previously described hollow cylinder was inserted a similar, but smaller, hollow cylinder with a closed top. This cylinder covered the open end of the pressure capillary which extended through the copper

support system into the sample chamber. A pressed indium O-ring seal was made between the base of this hollow cylinder and the top of the threaded plug. This seal was vacuum tight and prevented the sample gas from entering the pressure line when the chamber was being filled. Because this seal was easily broken when the pressure in the pressure capillary exceeded two atmospheres, it was possible to pressurize the inside of the bellows after it had been filled with the solid sample.

The copper supporting structure not only held the detachable copper piece, but also served as a support for a cylindrical copper "cage". The base of the supporting structure was threaded to fit similarly tapped threads in the base of the cage. The top of the cage contained the spring loaded, fixed plate assembly. To give this plate a fixed position, stops were machined a distance 0.317" from the top of the cage. The top of the cage was threaded to receive a 0.875" O.D. copper plate. Between this copper plate and the fixed plate was inserted a small spring. The spring was pliant enough so that a small pressure inside the bellows could lift the fixed plate above the stops in the cage, but was strong enough to insure that the plate returned to the stops when it was no longer in contact with the bellows.

The fixed plate consisted of a guard ring surrounded by a Mylar-insulated capacitor plate. The capacitor plate was made from a 0.486" O.D. copper piece with a 0.067" taper

per foot. This piece was wound with two layers of 0.001" Mylar and then pressed into a similarly tapered hole in a copper plate. The outside plate formed a guard ring for the capacitor plate.

The entire sample system was mounted on top of a steel pressure plug. The copper supporting structure was silver soldered to the steel plug at the point where the supporting structure passed through the steel plug. The outside of the pressure plug was threaded to fit the female threads of the pressure bomb. A 0.012" copper gasket was used to seal the pressure plug to a knife-edge surface machined into the bomb.

Steel was chosen as the material for the pressure bomb for two reasons. Firstly, the strength of steel permitted a minimal wall thickness of the pressure bomb. Secondly, the thermal expansion of steel is very nearly that for a ductile material such as copper which was to be used as the sealing gasket. If the gasket contracted more rapidly than the steel, then the bearing pressure on the sealing gasket would be appreciably reduced at low temperatures.

To permit easy access to the sample chamber, all electrical and capillary connections into the bomb were made through the pressure plug. The capacitor leads were attached to glass-to-metal seals which were soldered to the inside surface of the pressure plug.

As mentioned previously, the entire length of capillary to the top of the sample chamber had to be heated in order to fill the sample chamber. A stainless steel thermal standoff extended 2.5" from the outside surface of the pressure plug. The filling capillary was soldered to a feed-through glass-to-metal seal at the end of the thermal standoff. The capillary which was used to pressurize the pressure bomb was silver soldered into the pressure plug.

A large copper cylinder was soldered to that part of the sample support system which extended outside the pressure plug. Holes were drilled into this cylinder to form wells into which the thermometers were inserted. Apiezon type N grease was forced around the thermometers and into the wells to insure good thermal contact between the cylinder and the thermometers. All electrical leads were thermally anchored to this cylinder by soldering them to glass-to-metal seals set in the large copper cylinder. Capacitor leads were run on opposite sides of the sample support system, and,wherever unshielded, were separated as far as possible to reduce distributed capacitance. By disconnecting the leads at the capacitor plates, the distributed line capacitance was measured to be 0.004 pf. The distributed line capacitance affected the total capacitance by less than 0.4%. As mentioned previcusly, the capacitance leads were made from stainless steel and had a low temperature coefficient such that the change in the distributed line capacitance with temperature was essentially zero.

Temperature Measurements, Calibration, and Regulation

A "three-terminal" resistance bridge was used to measure the resistance of the germanium resistance-thermometer. A schematic drawing of the three-terminal resistance bridge is shown in Fig. 6. The term three-terminal means that the ground is important as well as the current leads to the unknown and standard resistor. By placing the current leads to the resistors across the ratio transformer and grounding the center tap of the ratio transformer, ground acts as a "guard point". At balance the detector signal is zero and no current is drawn. Therefore, any resistive or capacitive leakage to ground in the leads has no effect on the balance of the bridge. At balance, the unknown resistance of the germanium resistance-thermometer plus the lead resistance is given by

$$R = S\left(\frac{1 - x}{x}\right) , \qquad (15)$$

where R is the unknown resistance, S the resistance of the standard resistor, and x the reading of the ratio transformer. The use of stainless steel thermometer leads in the cryostat minimized both the temperature coefficient of the lead resistance and the total line resistance, while thermally isolating the sample system from room temperature.

The bridge was composed of a Model 120 PAR lockin amplifier with a fixed oscillator frequency of 400 Hz, a

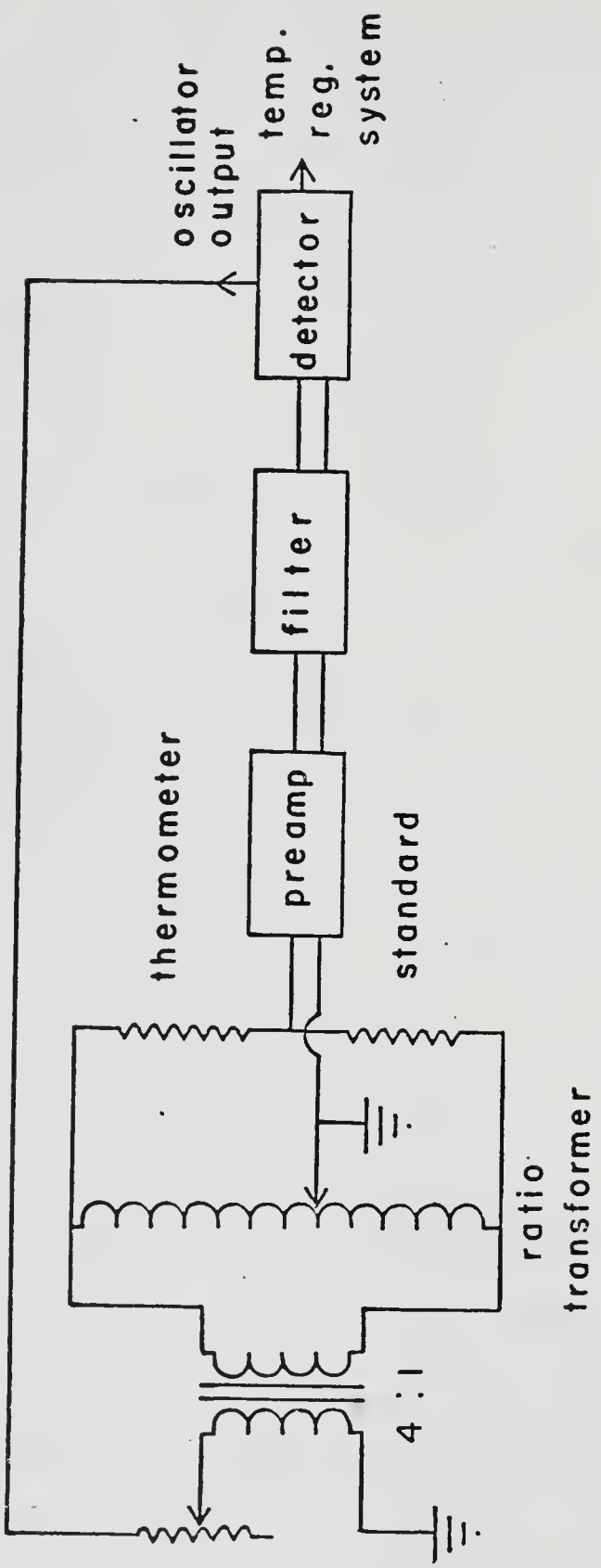

Fig. 6. Schematic drawing of three-terminal resistance bridge.

PAR CR4 differential preamplifier, a Gersch ST100-B isolation transformer, a Cryocal S/N 87 germanium resistance-thermometer, a wire-wound standard resistor (2000-ohms) with a low temperature coefficient, and a General Radio model 1493 ratio transformer.

The germanium resistance-thermometer was calibrated against both the vapor pressure of hydrogen and against a platinum resistance-thermometer. Between 12 and 20.4 K temperatures were calibrated against the vapor pressure of normal liquid hydrogen. All vapor pressure measurements were taken within three to four hours after condensation of the hydrogen gas into the vapor pressure bulb, and thus represented values appropriate for normal liquid hydrogen. The hydrogen was condensed into a copper bulb with a total volume of 2.5 cm^3. A strip of copper foil 0.010" thick, 0.50" wide and 10" long, was spiral wound to fit the inside of the chamber and was silver soldered to the bottom surface of the bulb. The large surface area provided good thermal contact between the liquid and the chamber.

In the temperature interval 10-77 K, the germanium resistance-thermometer was calibrated against a platinum resistance-thermometer, No. 1634579. This platinum thermometer had been calibrated in May, 1964 by the National Bureau of Standards.

For the germanium resistance-thermometer, if the log R is plotted against log T, the result is very nearly a straight line. To obtain temperatures between 4.2 and 10 K

this straight line was used to find the temperature ccrresponding to a measured value of the resistance. By using the average value, -.0591, for the slope of this line in the temperature interval 10-77 K, the temperature can be expressed as

$$T = \sum_{i=1}^{n} A_i R^{-0.591(i - 1)} , \qquad (16)$$

where R is the resistance, A_i the constants to be determined, and n the number of terms in the expansion. Since the resistance has already been expressed in terms of the bridge reading, the temperature is then given by

$$T = \sum_{i=1}^{n} A_i \left[\left[\frac{1 - x}{x} \right] 2000 \right]^{-0.591(i - 1)} . \qquad (17)$$

A program developed by Philp[35] permits the temperature to be calculated by computer directly from the bridge reading. This program gave a smooth temperature fit with a rms deviation of 0.02 K when five terms were used in the expansion.

To regulate the temperature, the out-of-balance signal from the lockin amplifier was used to heat the 1000-ohm coil wound on the inner vacuum jacket against the heat leak to the main bath. To maintain temperatures above 15 K, the output of the lockin amplifier was supplemented by a constant heating current supplied to the larger 5000-ohm coil also wound on the outside of the inner vacuum jacket.

Procedure and Sample Measurements

The sample gas was condensed into the sample chamber until the capacitance indicated that pressure was being

transmitted to the bellows. The liquid in the bellows was then cooled into the solid. A thermal gradient was established along the length of the chamber and more solid was sublimated from the filling capillary into the sample chamber. The heat needed to warm the capillary as well as the warm fluid entering the bellows from the capillary gradually raised the temperature of the entire sample system. The heat supplied to the capillary would then have to be reduced and the sample system allowed to cool much below the melting temperature of the sample. This process would be repeated until the capacitance and temperature indicated that the bellows was distended from its equilibrium position by the solid which it surrounded.

To insure that a good sample was formed, the sample was warmed above its melting point and allowed to cool slowly into the solid and then anneal for a period of from eight to ten hours. With the sample thus formed, the sample was cooled to 4.2 K over a two to three hour period.

To measure the expansion coefficient, heating and cooling curves of the capacitance as a function of temperature were taken. Near solid phase transitions, capacitance was measured at three to four millidegree intervals. Away from the solid phase transitions, capacitance was measured at 0.1 to 0.2 K intervals. Thermal equilibrium was indicated when the capacitance no longer changed at a fixed temperature. With the solid nitrogen samples, the temperature was maintained at 35.6 K for time periods ranging from one to three

hours to insure that the total length change associated with the first-order alpha-beta transition was measured accurately.

To measure the isothermal compressibility, the pressure bomb was pressurized with fluid helium. As mentioned previously, the fluid helium surrounded the sample as well as the sample chamber. The compressibility was measured by maintaining a constant temperature and noting changes in capacitance corresponding to changes in pressure. The pressure was varied by changing the height of the mercury in the U-tube. The pressure was read to 0.01 psi on a Texas Instruments pressure gauge.

IV. EXPERIMENTAL RESULTS AND DISCUSSION

The raw data obtained from these experiments consist of a series of values of capacitance corresponding to various temperatures at zero pressure, and a series of values of capacitance corresponding to various pressures at a fixed temperature. To relate the changes in capacitance to changes in length, we must first look at the expression for a three-terminal capacitor using a guard ring[36]

$$C = \frac{\pi \epsilon r^2}{l_g} + \frac{\pi \epsilon r w}{l_g + 0.22w}\left[1 + \left[\frac{w}{2r}\right]\right] , \qquad (18)$$

where C is the capacitance, ϵ the permittivity, r the radius of the plate with the guard ring, l_g the length between the capacitor plates, and w the half width of the distance between the inside radius of the guard ring and the outside radius of the capacitor plate surrounded by the guard ring. For w = 0.001", l_g = 0.020", and r = 0.486", the second term in the above expression affected the total capacitance by less than 1% and the ratio $\frac{1}{C}\left[\frac{dC}{dT}\right]$ by less than 0.4%.

To calculate the expansion coefficient, we find that a change in the gap length, dl_g, corresponding to a temperature change, dT, is given by

$$\frac{dl_g}{dT} = \frac{\pi \epsilon r^2}{C^2}\left[\frac{dC}{dT}\right] + \frac{2\pi \epsilon r}{C}\left[\frac{dr}{dT}\right] . \qquad (19)$$

Because the radial expansion of the copper capacitor plates is small, $\frac{1}{C}\left[\frac{dC}{dT}\right] \geq 10^4 \frac{1}{r}\left[\frac{dr}{dT}\right]$, the second term on the right-hand side of Eq. (19) shall be neglected. By noting that the change in the gap length is equal and opposite to the change in the sample length and that the coefficient of linear expansion is given by $\frac{1}{l_s}\left[\frac{dl_s}{dT}\right]$, we find that

$$\alpha_l = \frac{\pi \epsilon r^2}{l_s C^2}\left[\frac{dC}{dT}\right]. \qquad (20)$$

A correction to this term to be considered is the change in capacitance contributed by the expansion of the construction material. Because the entire sample system with the exception of the bellows was made from copper, only the expansion of copper over a length equal to the plate spacing plus the length of the sample had to be considered. A calculation of this correction showed that it affected the results by less than 0.5% and was well inside the scatter of the data.

A third correction to be considered was a correction for any tilt of one capacitor plate relative to the other capacitor plate. A relation developed by Philp[35] gives the correction to the expansion coefficient as

$$\alpha_{sample} = \alpha_{measured}\left[1 - \left[\frac{r^2\theta^2}{l_g^2}\right]\right], \qquad (21)$$

where r is the radius of the capacitor plate surrounded by the guard ring, θ the angle of tilt, and l_g the gap length at which the measurements of capacitance were taken. A measure of the effect of non-parallel plates was afforded

when the bellows, then filled with solid, became disengaged from the spring loaded capacitor plate. As the sample continued to cool, it was reasonable to assume that the shape of the sample would remain intact. A typical value of 48 pf was measured when the moving plate no longer touched the ground of the guard ring. This value of capacitance implied a plate spacing of less than 0.001" and therefore a $\theta = (0.001"/r)$. For a plate spacing of 0.020", this effect amounted to a correction of less than 0.07%.

To compute the expansion coefficient, the constant $\epsilon_o \pi r^2 l_s^{-1} = C_o$ was calculated and inserted into a computer program designed to determine the quantity $\frac{C_o}{C^2}\left[\frac{dC}{dT}\right]$. As has been mentioned, the temperature had been fitted by computer to a function of the bridge reading. Thus, with the exception of computing C_o, the computer calculated the expansion coefficient as a function of temperature from the raw data.

Because the fluid helium used to pressurize the sample also filled the space between the capacitor plates, the measured differences in capacitance caused by changes in pressure had to be corrected for the accompanying change in the dielectric constant of the fluid helium.

To calculate the isothermal compressibility, we find that a change in the sample length, dl_s, corresponding to a pressure change, dP, is given by

$$\left[\frac{dl}{dP}_s\right]_T = \frac{\pi \epsilon r^2}{C^2}\left[\frac{dC}{dP}\right]_T - \frac{\pi r^2}{C}\left[\frac{d\epsilon}{dP}\right]_T . \qquad (22)$$

Since $(dC/dP)_T$ is the quantity that is actually measured, we must calculate $(d\epsilon/dP)_T$ from published data.[37]

The dielectric constant, $K = \epsilon/\epsilon_o$, can be calculated for a given pressure and temperature by using the Clausius-Mosotti equation,

$$\alpha = \frac{3M}{4\pi\rho}\frac{(K-1)}{(K+2)} , \qquad (23)$$

in which α is the molar polarizability, M the molecular weight, and ρ the density. This equation has been verified[37] from above 300 K (gas) down to 1.62 K (liquid He II). Because the dielectric constant is equal to unity to within 1% over the pressure and temperature studied in this work, this equation may be rewritten as

$$K = \left[\frac{4\pi\alpha}{M}\right]\rho + 1 = 0.39\rho + 1 \qquad (24)$$

with ρ expressed in gm/cm^3. A change in permittivity corresponding to a change in pressure is then simply

$$\left[\frac{d\epsilon}{dP}\right]_T = \epsilon_o\left[\frac{dK}{dP}\right]_T = 0.39\epsilon_o\left[\frac{d\rho}{dP}\right]_T . \qquad (25)$$

Because the relative change in volume is three times the relative change in length, the expression for the isothermal compressibility becomes

$$K_T = \frac{3}{l_s}\left[\frac{dl_s}{dP}\right]_T = \frac{3\epsilon_o\pi r^2}{l_s}\left[\frac{K}{C^2}\right]\left[\frac{dC}{dP}\right]_T - \frac{0.39}{C}\left[\frac{d\rho}{dP}\right]_T . \qquad (26)$$

Because the density changed most rapidly with pressure at low temperatures, and the compressibility itself was a slowly varying function of temperature, the error in determining what fraction of the total capacitive change was due to a change in length of the sample was largest for the lowest temperatures.

Nitrogen

The Debye model for solids has been chosen for convenience in comparing the results of the present determination of the expansion coefficient and the isothermal compressibility with related quantities such as the specific heat and the velocity of sound in solid nitrogen. For a Debye solid, α, the expansion coefficient, and K_T, the isothermal compressibility, are related to C_v, the specific heat at constant volume, by

$$C_v = \frac{\alpha v}{K_T \gamma} \quad , \tag{27}$$

where γ is the Gruneisen parameter and v is the molar volume. The degree to which the ratio $\alpha v/K_T C_v$ varies from a constant is a measure of the specific applicability of this model to nitrogen and will be discussed later in terms of the temperature dependence of the Gruneisen parameter.

The temperature dependence of the specific heat at zero pressure for solid nitrogen is depicted in Fig. 7. Comparison of the specific heat measurements given in Fig. 7 to the temperature dependence of the relative changes in length of nitrogen shown in Fig. 8 suggests that not only is there an abrupt change in the lattice size corresponding to a change in structure, but also that the lattice must expand rapidly in the alpha phase near the transition

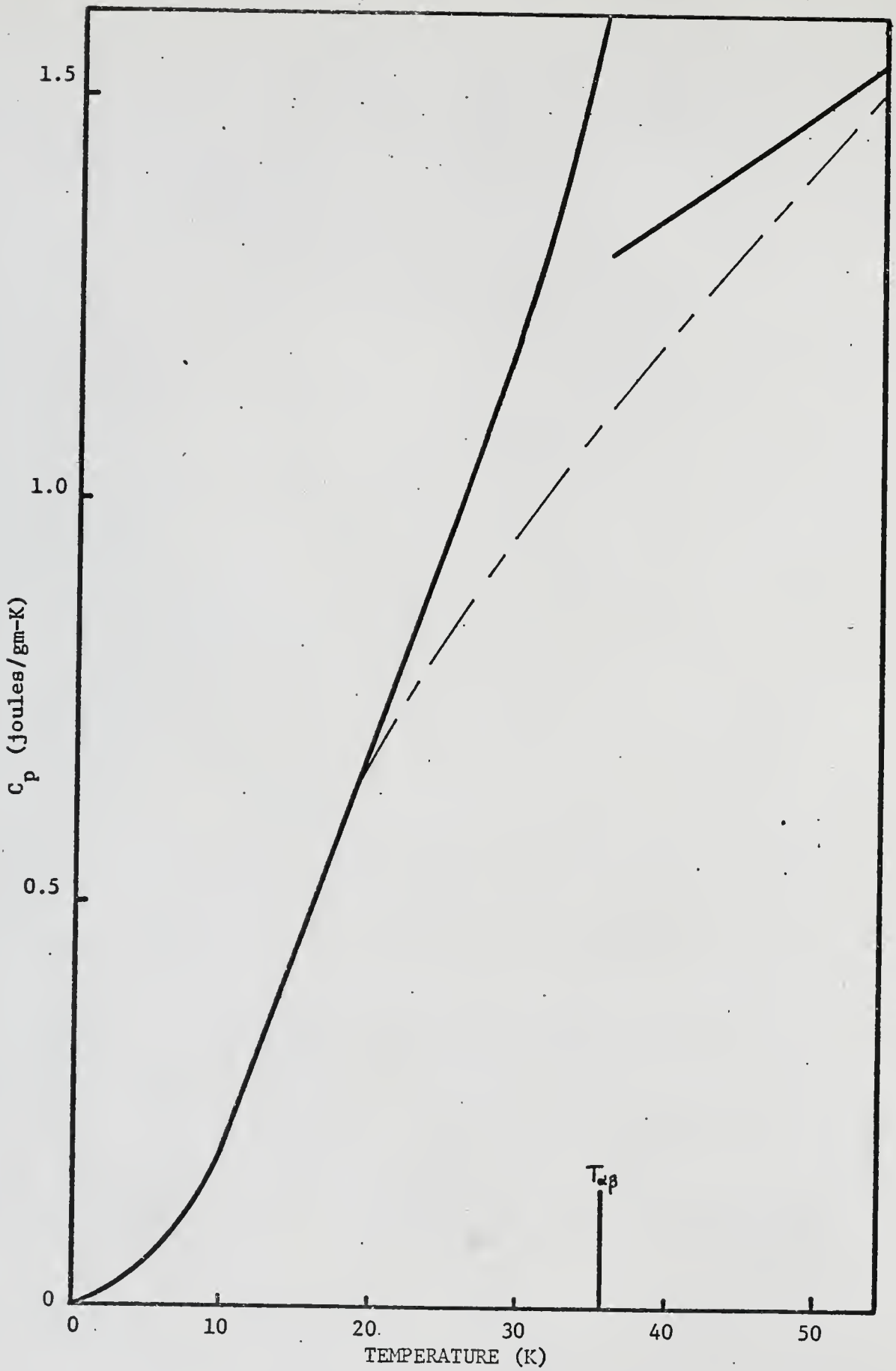

Fig. 7. Specific heat versus temperature for solid nitrogen. Dashed curve represents behavior expected from a Debye solid with θ_D = 80K.

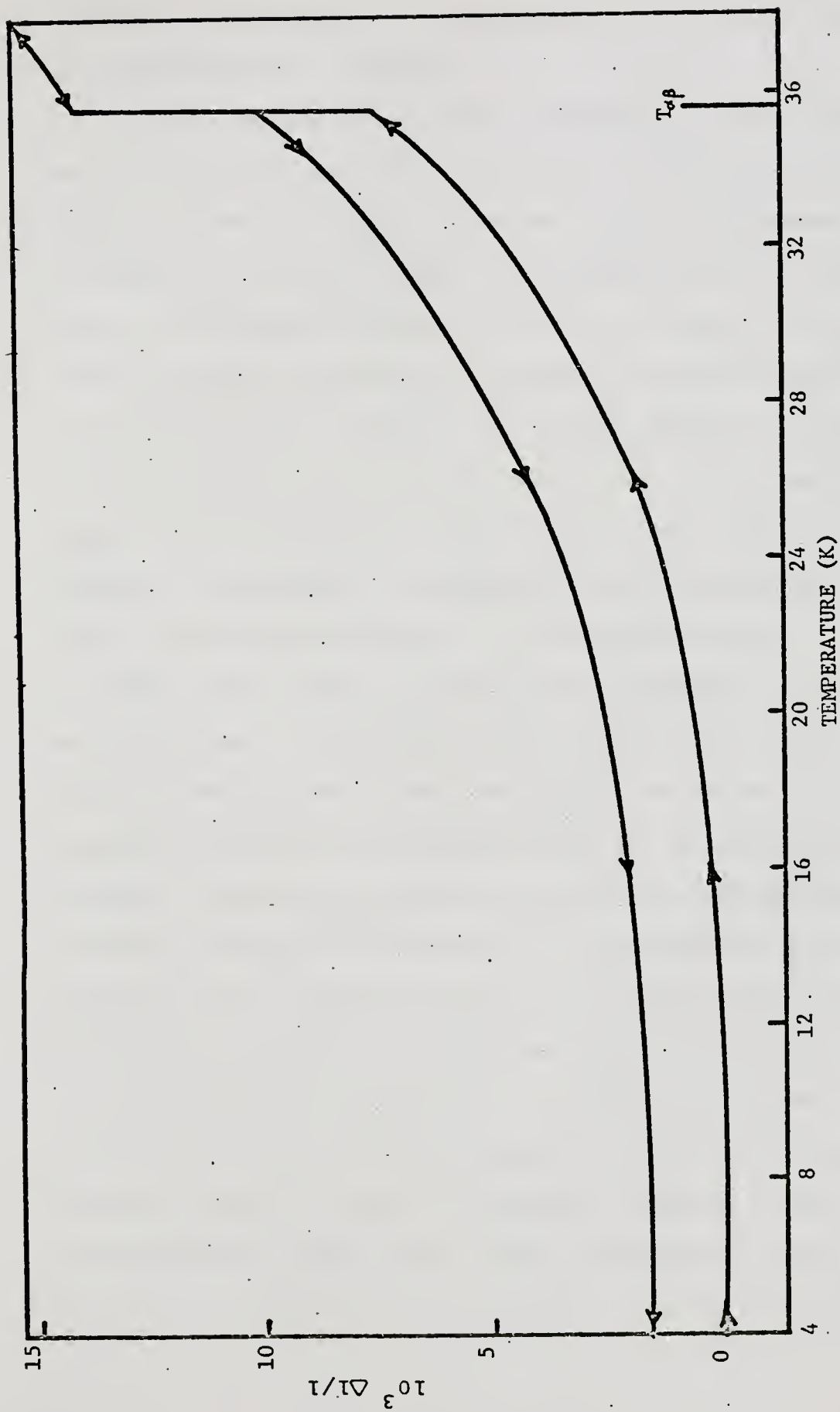

Fig. 8. Relative length changes versus temperature for solid nitrogen. Arrows indicate warming and cooling values. The scatter in the data is less than the width of the line drawn in the figure.

in order to accommodate the large amount of energy given to the solid as it is warmed.

Recent thermal expansion measurements by MTV[10] give the relative change in volume at 35.6 K as 0.5%, which is lower than the 0.8% value obtained earlier by Swenson.[1] The magnitude of this change as determined by this work gave a 1.4% change on warming and a 0.9% change on cooling. Several efforts were made to reconcile the difference in volume change when warming and cooling through the transition. After cooling to initiate the transition, the transition temperature was maintained for two to three hours. The length of the sample, as detected by the capacitance bridge, would change for the first hour, after which time no change in length would occur as long as the transition temperature was maintained. Cooling below the transition produced a thermal contraction of the same magnitude as the thermal expansion observed when warming through the same temperature interval. Thus, there was no evidence of supercooling. An analogous approach to determine if superheating had occurred also produced a negative result. MTV also noticed the presence of hysteresis in the vicinity of the phase transition.

The ratio $\Delta l/l$ versus $1/T$ is shown in the semilogarithmic plot given in Fig. 9. By choosing T_1 as absolute zero, the slope of $\ln(\Delta l/l)$ versus $1/T$ remains constant from 24 K to the transition temperature. From the slope of this line an activation energy of 300 cal/mole was calculated from

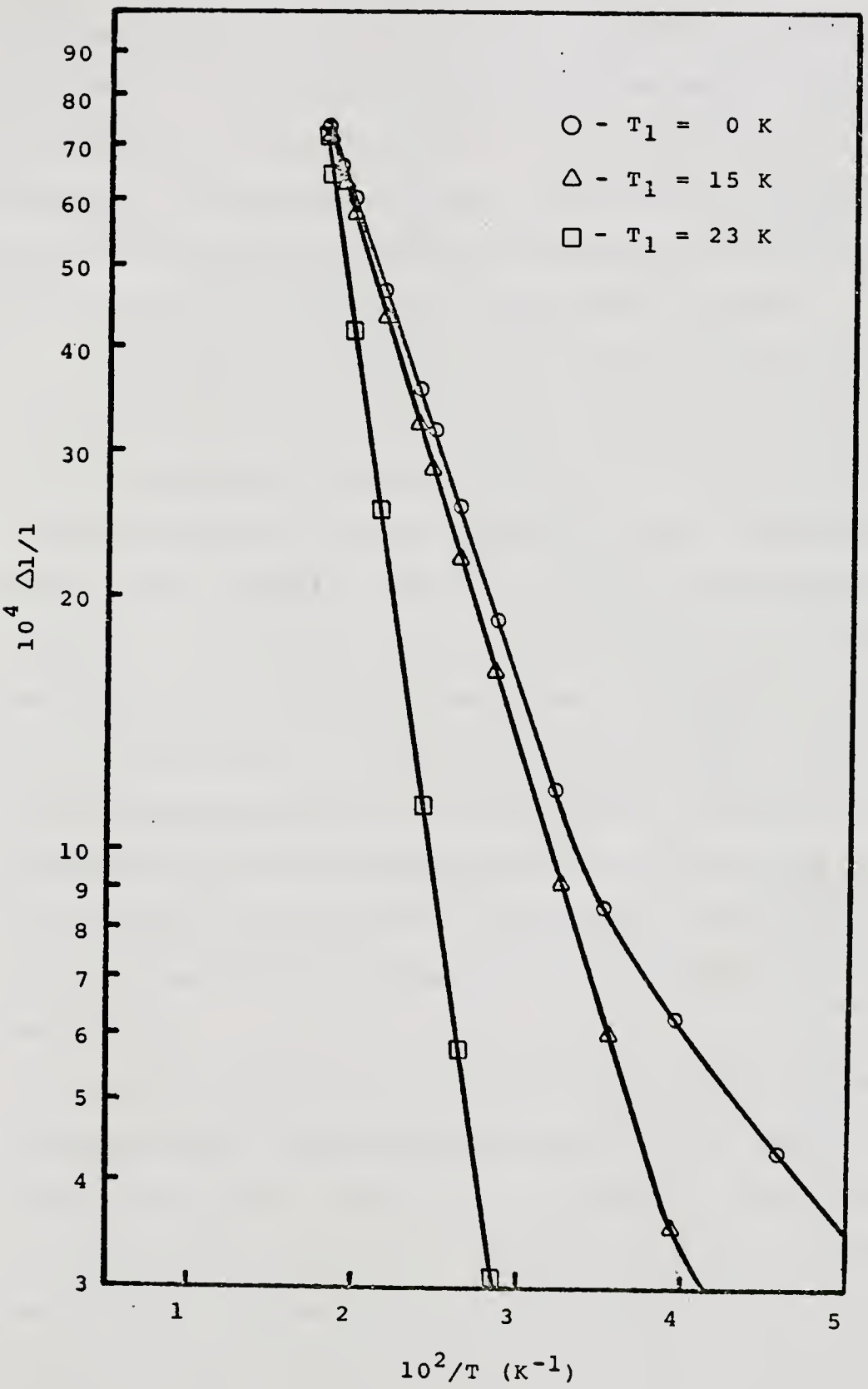

Fig. 9. Semilogarithmic plot of relative length changes versus inverse temperature for alpha nitrogen.

Eq. (12) in Chapter II. By choosing T_1 = 15 K, the slope remains constant from 20 K to the transition temperature and gives an activation energy of 310 cal/mole. Finally, by choosing the same T_1 as MTV, T_1 = 23 K, an activation evergy of 370 cal/mole was found. This is to be compared with the 450 cal/mole activation energy found by MTV and the 460 cal/mole activation energy found by BKMP.

The temperature interval for which the slope remains constant found in this work is much larger than that found by MTV and compares favorably with the 24-35.6 K interval in which the excess specific heat has been attributed to orientational defects. This is also the same temperature interval in which the pure quadrupole resonance frequency has been found to obey the parameter relation given in Eq. (8) in Chapter II. While the data do seem to obey the postulated behavior for orientational defects, it is apparent from the differences found in calculating activation energies corresponding to different choices of T_1 that the experimental evidence of such behavior is far from conclusive.

A point-by-point differentiation of length changes corresponding to temperature changes gave the expansion coefficient shown in Fig. 10. The scatter in the data is a reflection of the limit of capacitive and temperature sensitivity. As can be seen from the reproducibility of the heating and cooling curves in both Fig. 8 and Fig. 10, thermal equilibrium was established for all measurements.

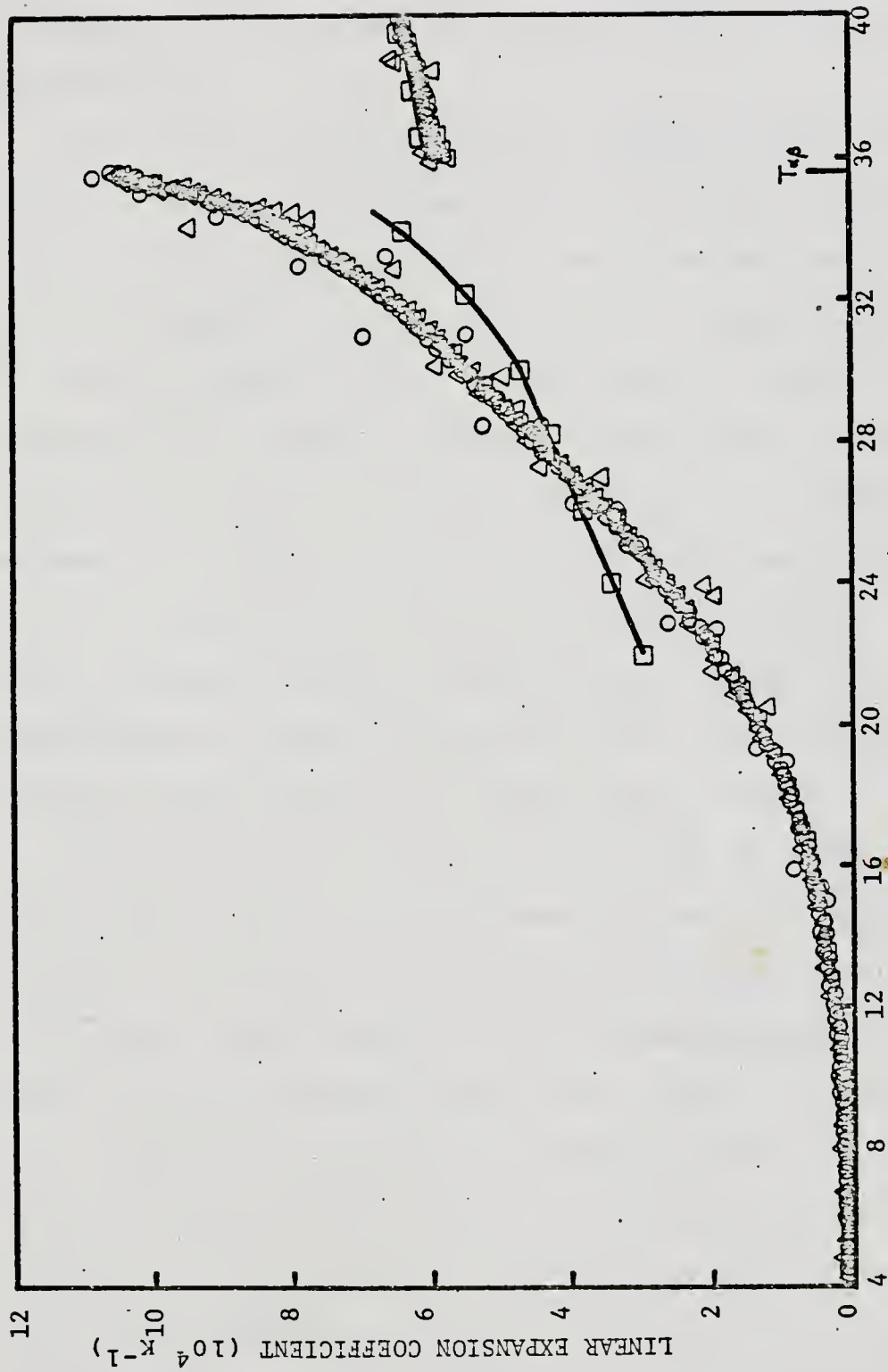

Fig. 10. Linear expansion coefficient versus temperature for solid nitrogen. O's and Δ's represent data points taken when warming and cooling the sample. □'s represent data points given by MTV, Ref. 10.

The expansion coefficient is discontinuous at 35.6 K, as is the specific heat, and the temperature dependence of the expansion coefficient is similar to that of the specific heat.

Also shown in Fig. 10 are the results of MTV. As mentioned before, the measurements of MTV near the phase transition exhibited hysteresis and no thermal expansion data were reported from 34.5 to 36.5 K. Experimentally the results quoted by MTV represent length changes measured over 1 and 2 K intervals, except near the phase transition, where measurements were taken over 0.25 K intervals. Since no mention is made by MTV about their limit of resolution in detecting changes in length, it is fair to assume from the relatively small expansion coefficient of alpha nitrogen that the large temperature intervals were required to detect length changes.

Because length changes were measured over smaller temperature intervals in this work, it is not surprising to find that this determination of the expansion coefficient gave smaller values for α_1 at lower temperatures and larger values for α_1 at higher temperatures. What is surprising is the degree to which the two results differ. The lowest data point given by MTV at 21 K is 30% higher than that measured in this work. The highest data point given by MTV in the alpha phase of solid nitrogen at 34.5 K is 26% lower than that found in this work. The differences in these results become more acute when we consider the Gruneisen

parameter, but to compute the Gruneisen parameter we must first determine the isothermal compressibility of solid nitrogen.

The isothermal compressibility, as measured in this work, and the adiabatic compressibility as measured by BTI[11] are shown as a function of temperature in Fig. 11. The isothermal compressibility, K_T, is related to the adiabatic compressibility, K_S, as given by Eq. (1) in Chapter I. To compare the measured values of the adiabatic compressibility with measured values of the isothermal compressibility, the following three curves are also plotted in Fig. 11. The first curve is the adiabatic compressibility and was calculated from the isothermal compressibility and thermal expansion measured in this work. Agreement with the measured values of BTI at temperatures near the transition is good, but the agreement becomes worse as the temperature decreases. The second curve is the isothermal compressibility as calculated from the adiabatic compressibility measured by BTI and the expansion coefficient measured by MTV. Agreement with the isothermal compressibility measured in this work is good at low temperatures, but becomes poorer as the alpha-beta transition is approached. The third curve is the isothermal compressibility as calculated from the measurements of the expansion coefficient given in this work and from the measurements of the adiabatic compressibility given by BTI. Agreement with the measured isothermal compressibility

Fig. 11. Measured and calculated compressibilities for solid nitrogen.

- ○ Isothermal compressibility measured in this work.
- ◇ Adiabatic compressibility measured by BTI, Ref. 11.
- ○ Isothermal compressibility as calculated from the adiabatic compressibility measured by BTI and the expansion coefficient measured in this work.
- △ Adiabatic compressibility as calculated from the isothermal compressibility and expansion coefficient as measured in this work.
- □ Isothermal compressibility as calculated from the adiabatic compressibility as measured by BTI and the expansion coefficient as measured by MTV, Ref. 10.

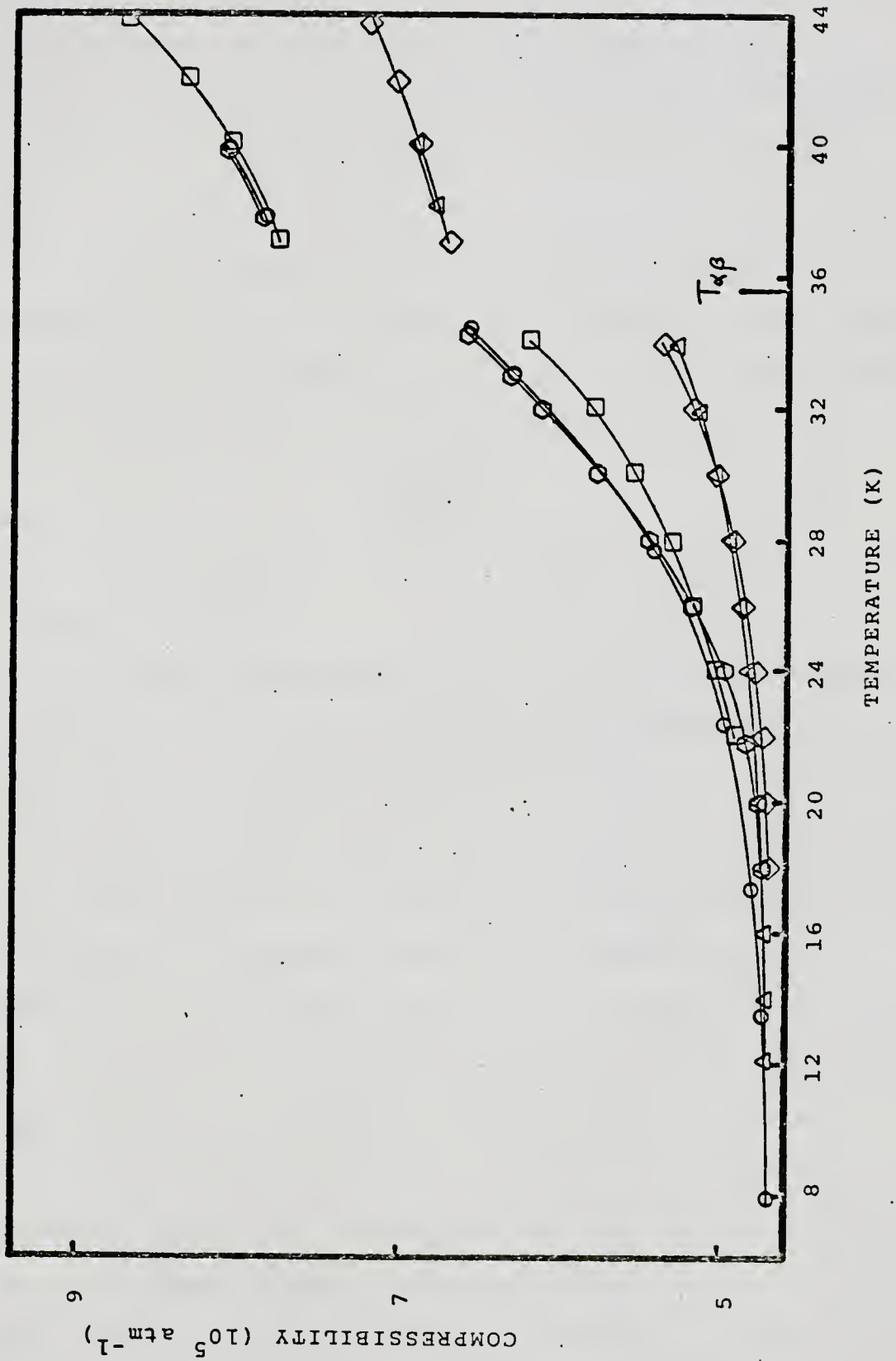
COMPRESSIBILITY (10^5 atm^{-1})
6
7
5
8
12
16
20
24
28
32
36
40
44
$T_{\alpha\beta}$
TEMPERATURE (K)

is excellent from 28 K to the transition temperature, but at temperatures less than 28 K the agreement becomes poorer. In any event, the worst disagreement between the measured and calculated compressibilities is less than 2%.

Having determined the isothermal and adiabatic compressibility of solid nitrogen in its alpha phase, the specific heat at constant volume, C_v, can be simply related to the specific heat at constant pressure, C_p, as

$$C_v = \left[\frac{K_S}{K_T}\right] C_p \quad . \qquad (28)$$

Having found C_v, the Gruneisen parameter can now be calculated.

The temperature dependence of the Gruneisen parameter was calculated from Eq. (27) using the isothermal compressibility and the expansion coefficient measured in this work. The temperature dependence of the Gruneisen parameter was also calculated using the adiabatic compressibility measured by BTI and the expansion coefficient measured by MTV. These results are shown in Fig. 12. As can be seen in Fig. 7, above 20 K the behavior of the specific heat for alpha nitrogen is markedly different from that expected for a Debye solid. It is not clear how the Gruneisen parameter can remain constant over a temperature interval where the specific heat differs appreciably from that of a Debye solid. Yet, the Gruneisen parameter as calculated from the measurements of BTI and MTV would seem to indicate that alpha nitrogen is nearly a perfect Debye solid.

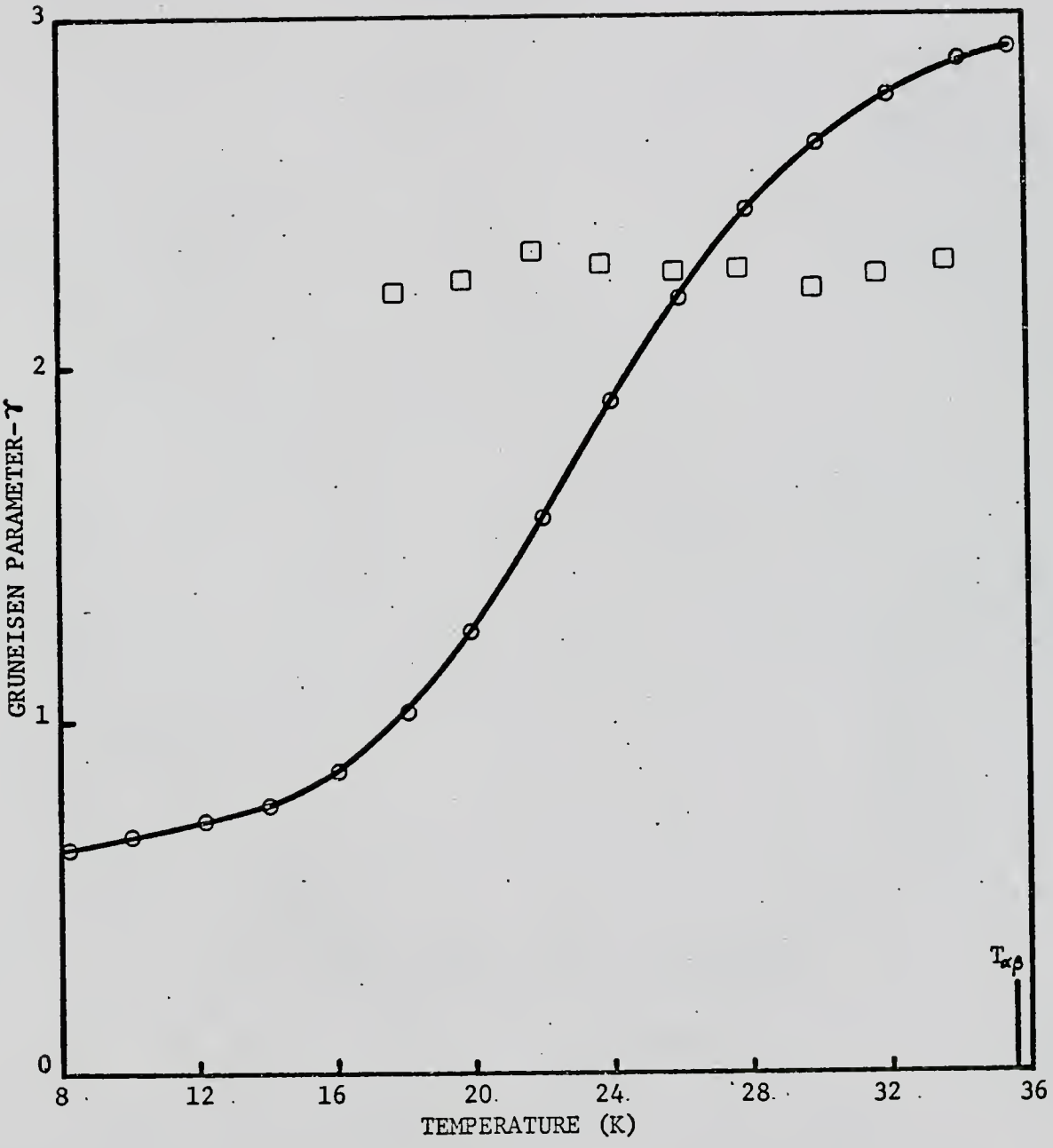

Fig. 12. Gruneisen parameter versus temperature for alpha nitrogen. □'s represent values calculated from measurements of MTV and BTI, Refs. 10 and 11.

The Gruneisen parameter as calculated solely from the results found in this work is more easily understood. Clearly, the Debye model predicts no first-order phase change at any temperature below the Debye temperature, θ_D. The degree to which the Gruneisen parameter varies can be considered a measure of how a particular solid deviates from the behavior of an ideal Debye solid. As can be seen from Fig. 12, the Gruneisen parameter has a strong temperature dependence as the transition temperature is approached.

From the nearly constant behavior of γ below 18 K found in this work, alpha nitrogen can be said to behave like a Debye solid in the so-called "T^3" region. There is some question as to the absolute magnitude of γ as found in this work, because one would nominally expect to have a value between 1 and 2. It is not clear, however, what shape the expansion coefficient would have to assume from 0 to 20 K to maintain a higher value for the Gruneisen parameter.

Methane

The specific heat of solid methane as measured by Clusius[6] is shown in Fig. 13. The solid undergoes a change of phase at 20.4 K as is evidenced by the large λ anomaly in the specific heat.

Relative length changes in methane measured in this work are shown in Fig. 14. The reproducibility of the

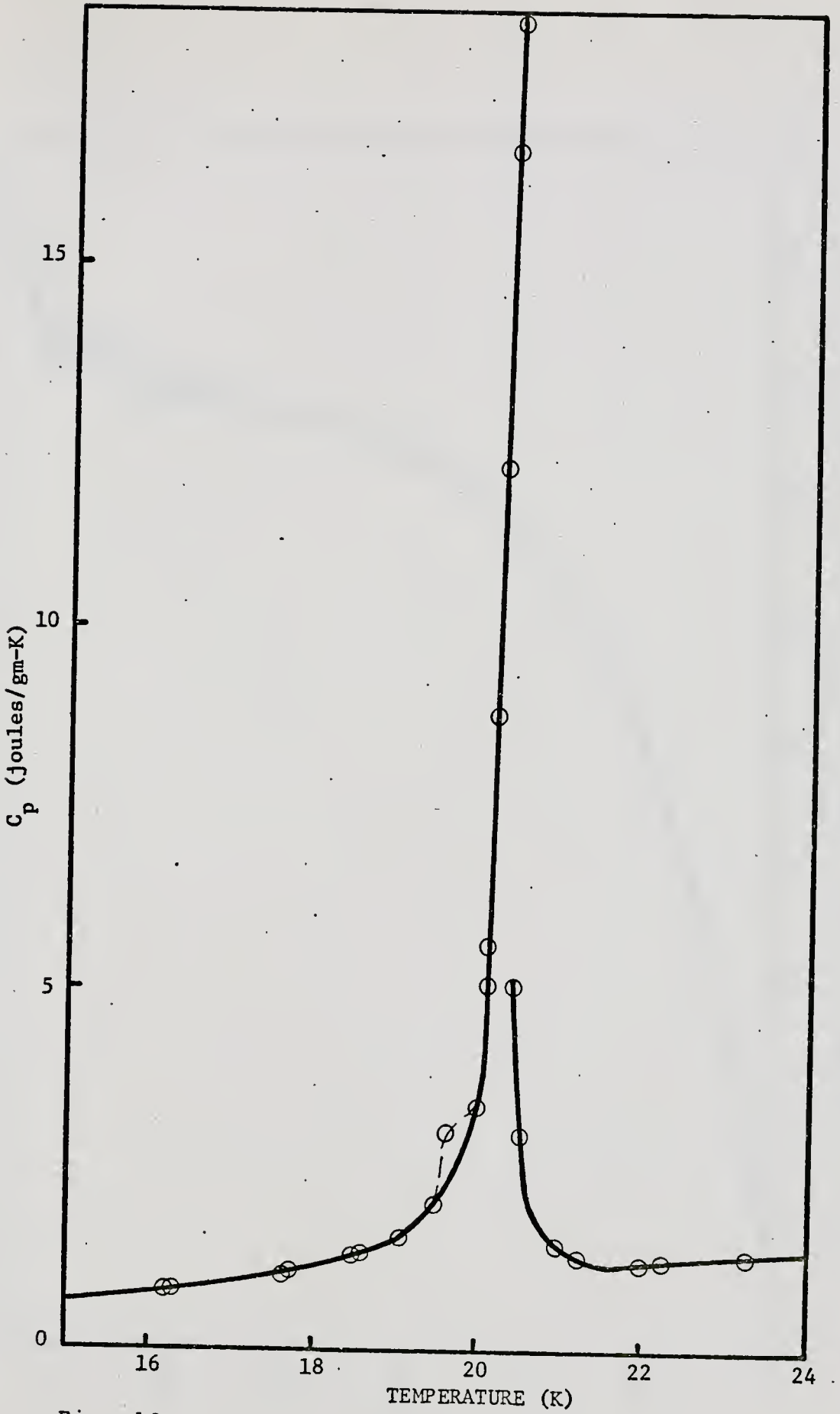

Fig. 13. Specific heat versus temperature for solid methane. O's represent data points given by Clusius, Ref. 6.

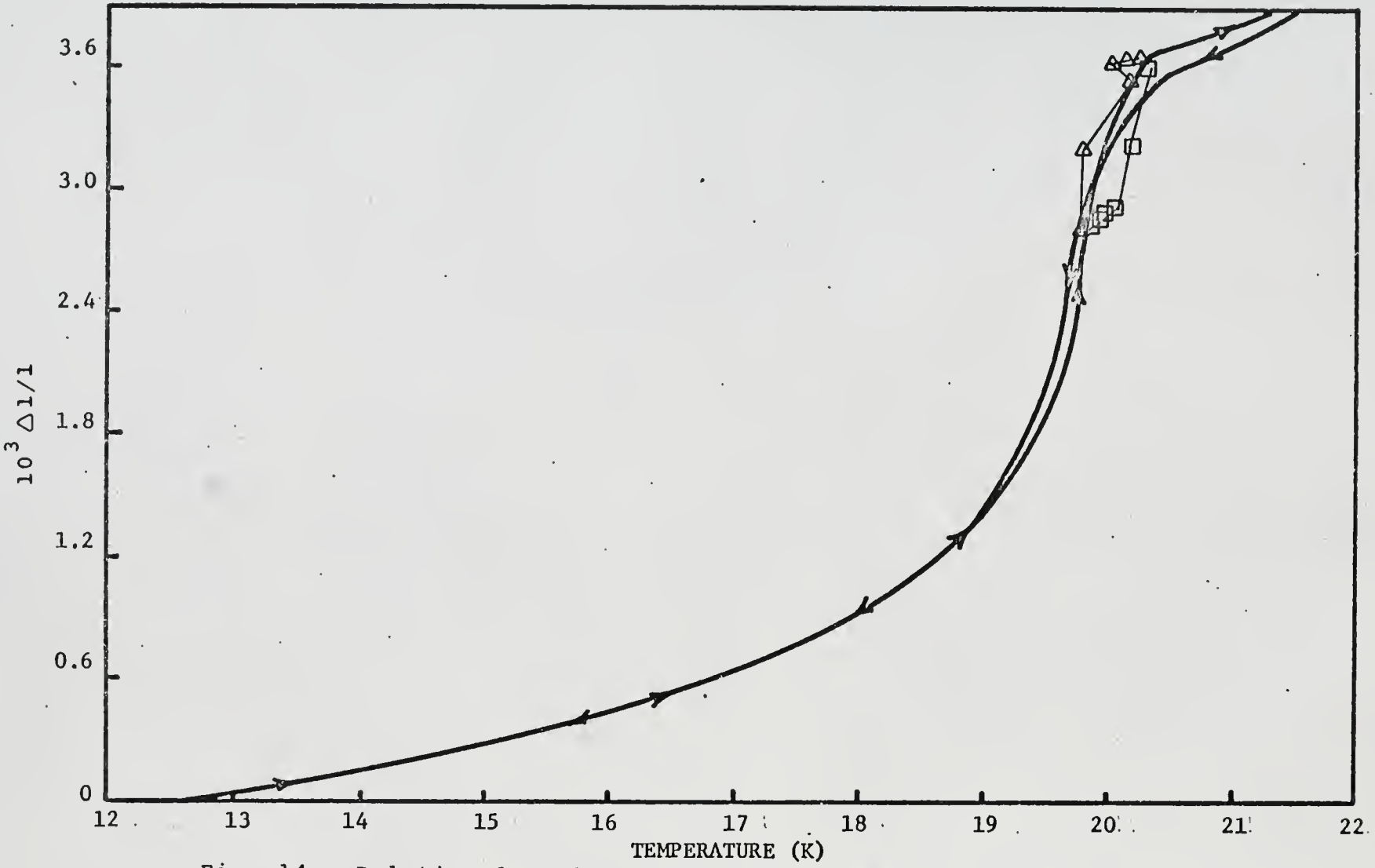

Fig. 14. Relative length changes versus temperature for solid methane. Arrows indicate warming and cooling values. The scatter in the data is less than the width of the line drawn in the figure. △'s and □'s represent the cooling and warming values found by Heuse, Ref. 20.

warming and cooling curves establishes that all points were taken in thermal equilibrium. Fast heating rates displaced the warming curves to higher temperatures. Also shown in Fig. 14 are the warming and cooling curves found by Heuse.[20] It is important to note the similarities in the results of Heuse and the results presented in this work. The transition is spread out below 20.4 K with the consequence that neither result gives a maximum slope at 20.4 K. Furthermore, while $\Delta l/l$ remains continuous, dl/dT is discontinuous at 20.4 K.

The expansion coefficient of methane as measured in this work is shown in Fig. 15. The circles and triangles represent two samples of different length and formed from different gas. The maximum in the expansion coefficient is found to be at 19.8 K. It is also apparent that at 20.4 K the solid is entirely in the higher temperature phase. Also shown in Fig. 15 are the thermal expansion measurements of MTV.[10] Unfortunately, MTV reported no measurements below 22 K.

If for some reason the temperature calibration was grossly in error, a determination of the specific heat would show a maximum at a temperature different from that given by the calibration. A crude determination of the specific heat was effected by making simultaneous measurements of the temperature and length changes at equal time intervals when heating at a slow constant rate. The temperature dependence of the expansion coefficient remained the same, but the maximum slope in the time versus temperature plot, shown in

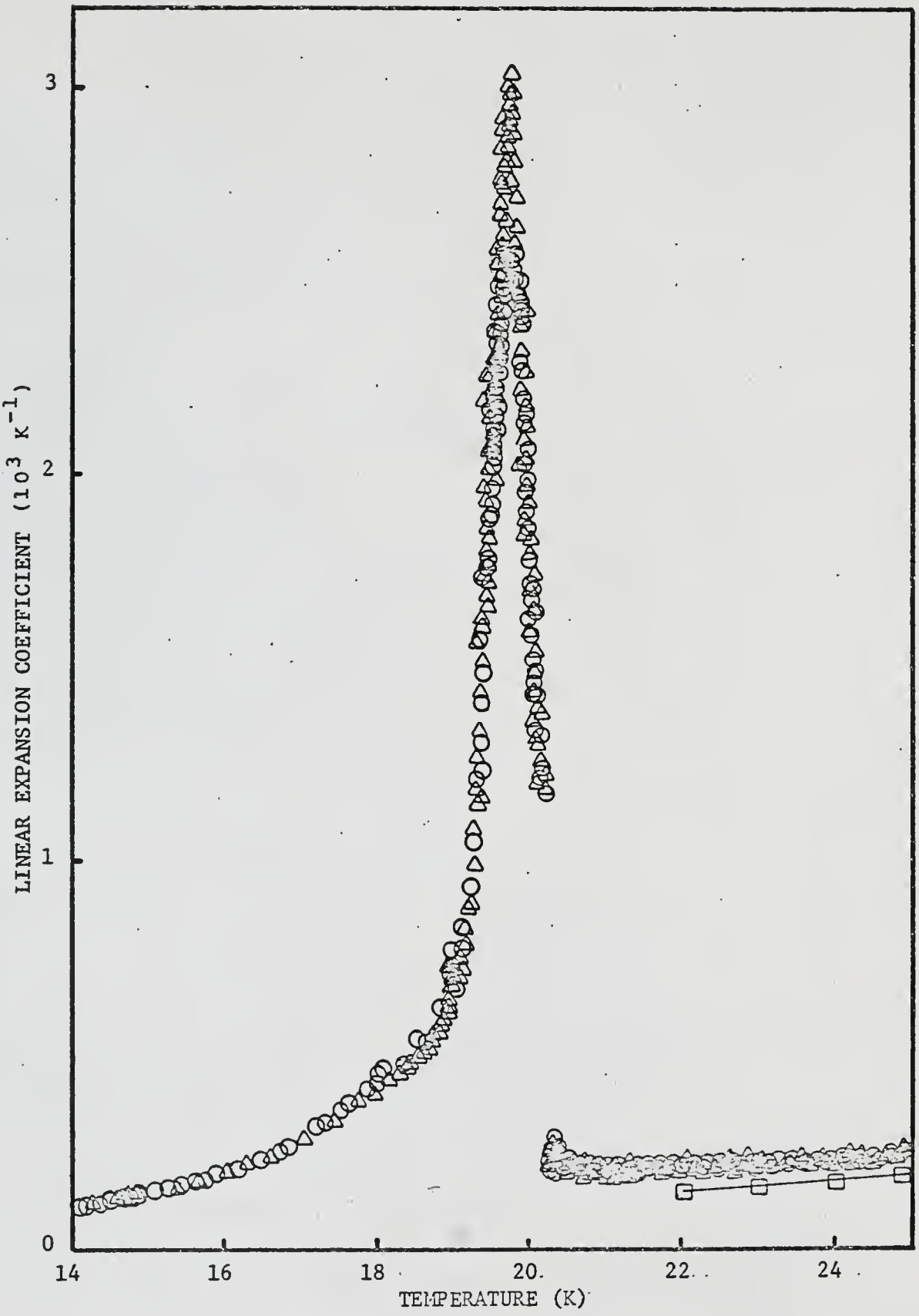

Fig. 15. Linear expansion coefficient versus temperature for solid methane. ○'s and △'s represent values for two different samples. □'s represent data points given by MTV, Ref. 10.

Fig. 16, occurred at 20.4 K. The specific heat at constant pressure is proportional to dt/dT, which we shall call C_p'. A plot of C_p' versus temperature is shown in Fig. 17. Since points were taken at five minute intervals, the detailed structure of the specific heat near 20.4 K could not be determined. It is now obvious that the temperature calibration was not in error, and that the temperatures at which the specific heat and the expansion coefficient are maxima are indeed different.

To explain the difference in the temperature at which the specific heat is a maximum and the temperature at which the expansion coefficient is a maximum, let us consider the general thermodynamic relation

$$C_p = C_v + \alpha^2 TvK_T^{-1} \quad . \qquad (29)$$

Eq. (29) is a different way of expressing Eq. (1) given in Chapter I. If it is assumed that C_v is a smoothly-varying function of temperature and that for small values of the expansion coefficient C_v is approximately equal to C_p, then any "bump" in C_p must be attributed to the term $\alpha^2 TvK_T^{-1}$. At 19.8 K, where the expansion coefficient is a maximum, the magnitude of this term is 1.37 cal/mole-K. The specific heat, as measured by Clusius[6] and given in Fig. 13, exhibits a small bump at 19.8 K with a height of approximately 1.6 cal/mole-K above that assumed to be contributed by C_v. These two quantities are in reasonable agreement. Rosenshein[16] reported double peaks in the specific heat in all the upper transitions which he measured. The smaller peak usually

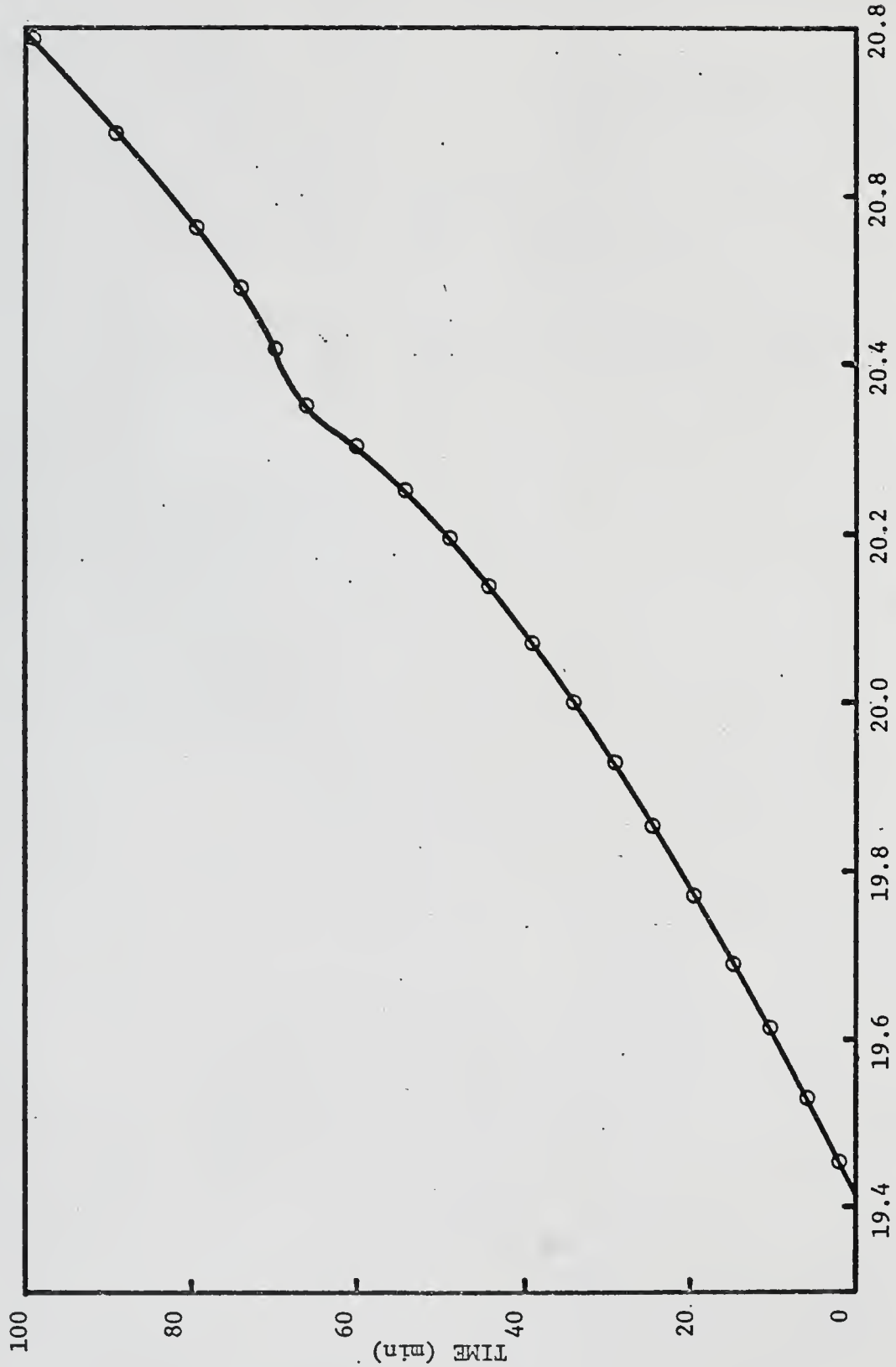

Fig. 16. Time versus temperature for a typical warming curve of solid methane.

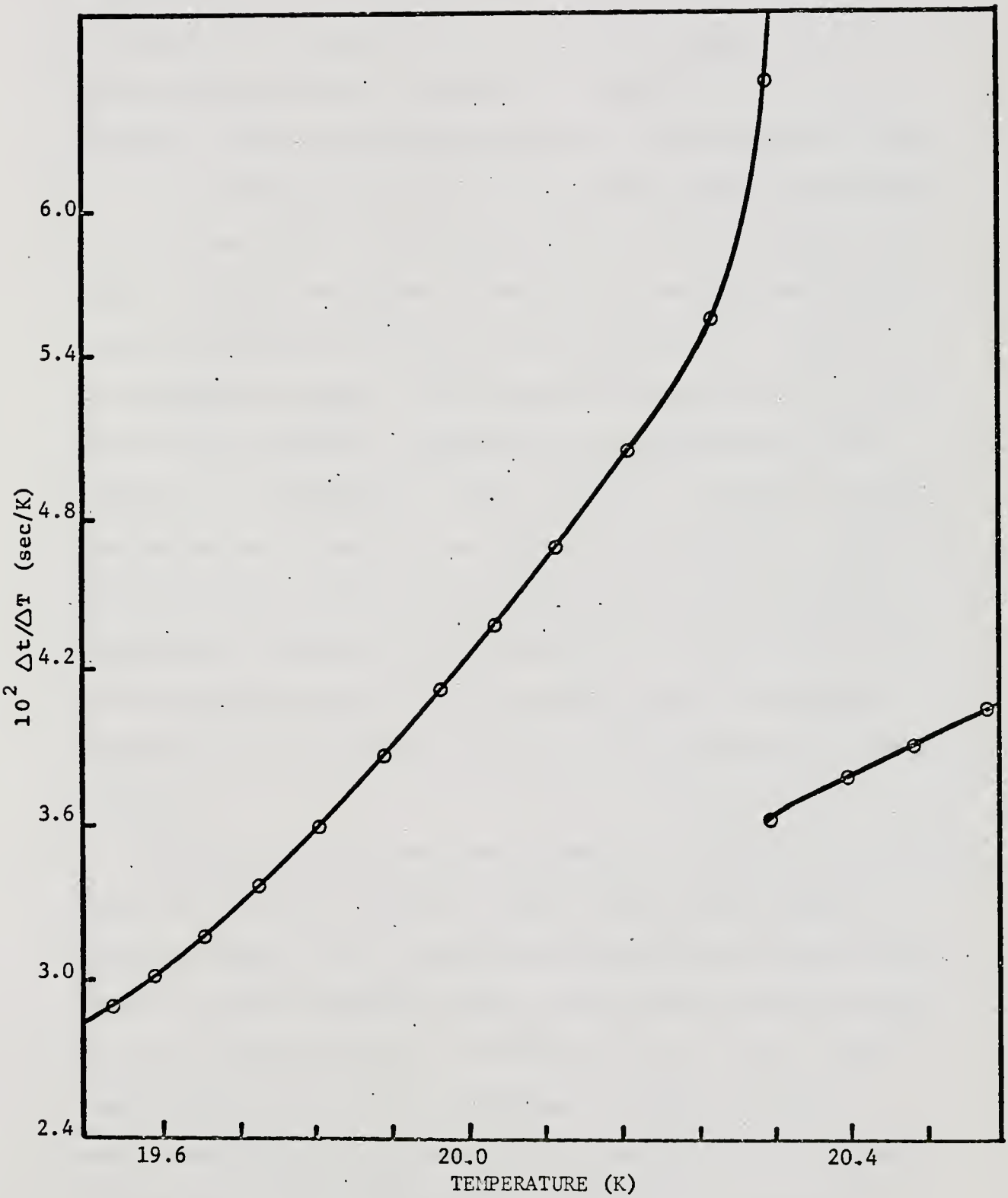

Fig. 17. Specific heat (C_p') versus temperature for solid methane.

occurred 0.25 K below the main peak in the specific heat. While the specific heat measurements reported in this work were much too crude to resolve and confirm this structure in the specific heat at 19.8 K, it does appear that the expansion coefficient measured in this work is not at variance with existing measurements of the specific heat.

It is also helpful to look at the general properties of the transition. The transition is of the cooperative type, in which the modes of motion of each molecule are directly affected by those of its neighbors. There is no noticeable change in the crystal structure at 20.4 K, but as the transition temperature is approached, each molecule is reoriented in the lattice. In order for this reorientation to occur, the lattice must expand. From the results of this work, it appears that the greater part of the lattice expansion occurs before 20.4 K and that most of the energy assumed by the lattice goes into the new rotational modes allowed for the new orientation of each molecule.

Recent specific heat measurements by CGM,[19] which are shown in Fig. 18, exhibit a broad excess heat capacity centered about 8 K. Because equilibriation times become longer at lower temperatures, varying from several hours at 5 K to approximately 20 minutes at 11 K, only a few experimental points were reported by CGM. Specific heat measurements by Rosenshein[16] have shown the presence of a second, lower temperature transition to pressures

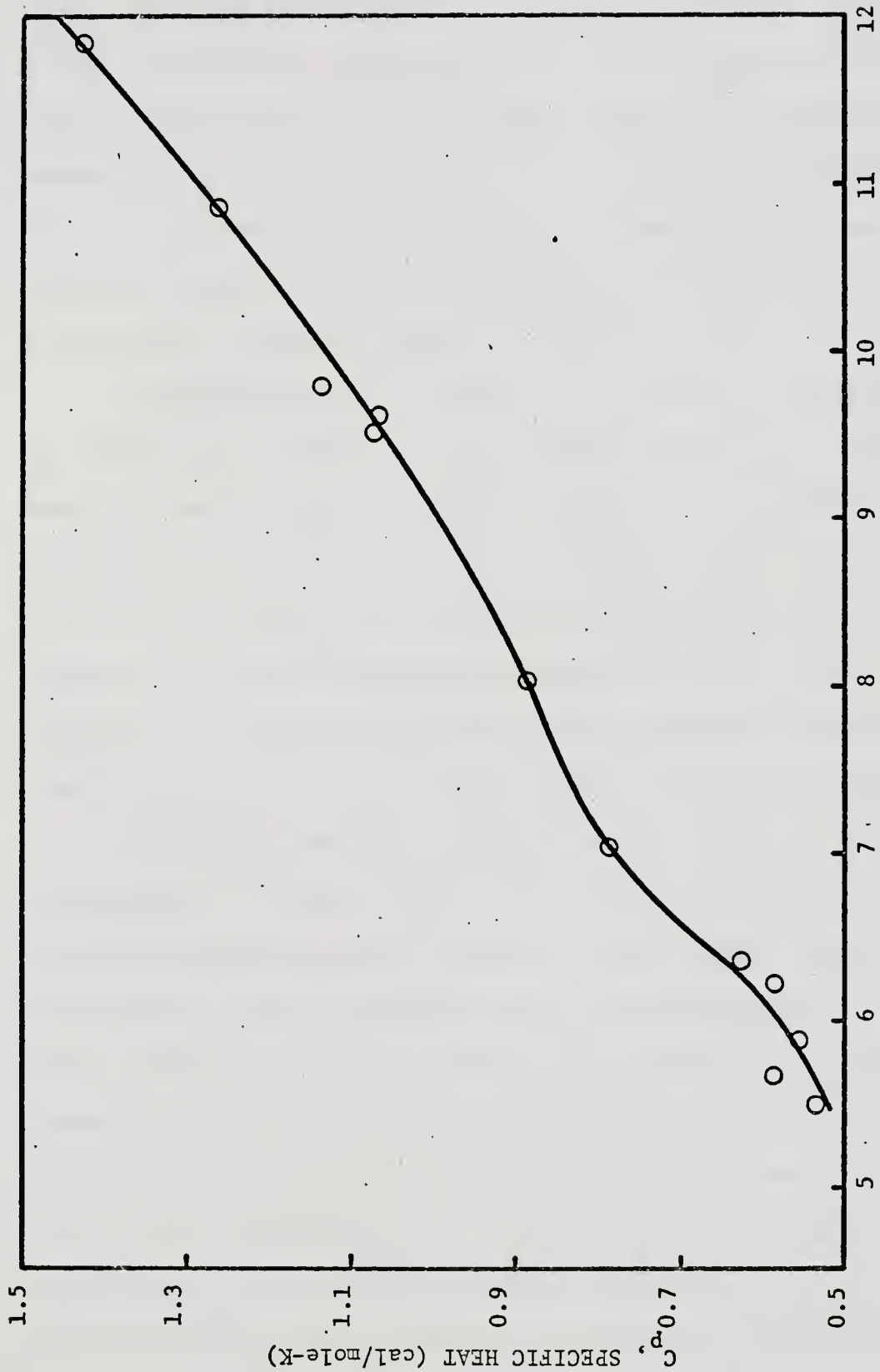

Fig. 18. Specific heat versus temperature for solid methane at low temperatures. O's represent data points given by CGM, Ref. 19.

as low as 200 atm. An extrapolation of the lower temperature phase boundary determined by Rosenshein to zero pressure gives a transition temperature of 9.5 K. Because the transition becomes broader at low temperatures, the agreement is reasonable. It must be pointed out, however, that there is no other experimental evidence to verify that the high pressure phase observed by Rosenshein is the same as the excess heat capacity found by CGM.[19]

Relative changes in length as a function of temperature as determined in this work are shown in Fig. 19. It is readily apparent that negative expansion occurs below 8.75 K. Calculation of the expansion coefficient does not clarify the issue. In fact, the expansion coefficient as calculated from Fig. 19 has a negative minimum at 7.5 K. It is difficult to compare this behavior to existing specific heat measurements in any other than a qualitative manner.

Attempts to explain the long equilibriation times and the peculiar thermal behavior below 12 K in terms of hydrogen spin conversion are inconclusive. The sample apparently does reach thermal equilibrium, as was evidenced in this work. The length of the sample, as measured by the capacitance, would change rapidly when warmed or cooled. The length would continue to change slowly when the temperature was held at the new value. Thermal equilibrium was established in a time related to the temperature. As was noticed by CGM, the lower the temperature, the longer the equilibriation time. Attempts to ascribe a rate constant

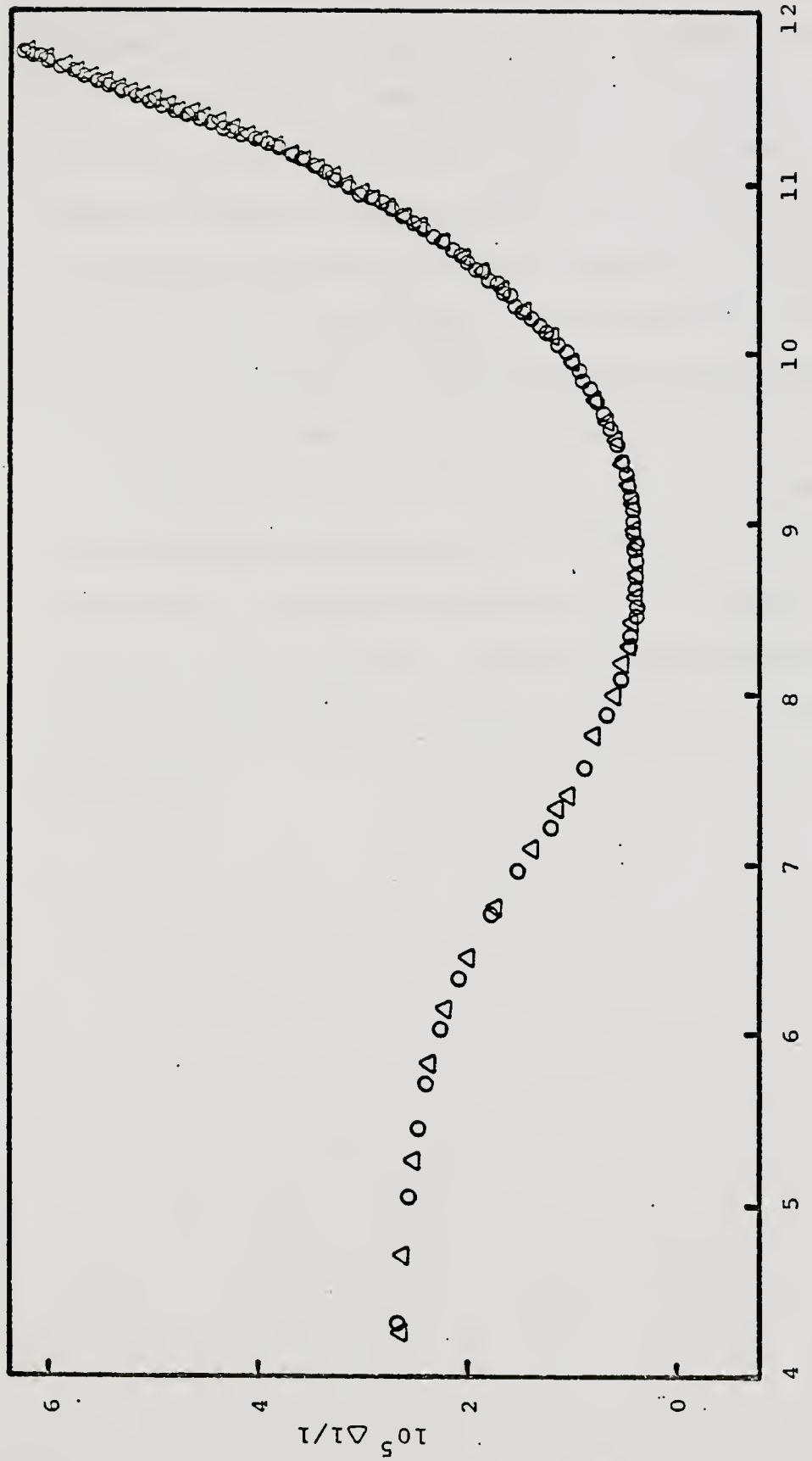

Fig. 19. Relative length changes versus temperature for solid methane at low temperatures. O's and Δ's represent data points taken when warming and cooling the sample.

to the equilibriation time similar to that found for ortho-para conversion in liquid and solid hydrogen were unsuccessful. If conversion were taking place, it would have been an irreversible process, as in liquid and solid hydrogen where the para hydrogen becomes frozen in the lattice. If the negative expansion observed below 8.75 K were caused by spin species conversion, then by warming the sample to a higher temperature, the conversion would continue to occur and the sample would continue to expand. The results of Fig. 19 do not bear this out. It would appear that the best approach to determine the nature of the low temperature properties of solid methane would be to make more sensitive specific heat or thermal expansion measurements at pressures up to the lower limit of the phase boundary determined by Rosenshein.

REFERENCES

1. C. A. Swenson, J. Chem Phys. 23, 1963 (1955).

2. L. H. Boltz M. E. Boyd, F. A. Mauer, and H. S. Reiser, Acta Cryst. 12, 247 (1959).

3. T. H. Jordan, H. W. Smith, W. E. Streib, and W. N. Lipscomb, J. Chem Phys. 41, 756 (1964).

4. W. E. Streib, T. H. Jordan, and W. N. Lipscomb, J. Chem. Phys. 37, 2962 (1962).

5. A. L. Smith, W. E. Keller, and H. L. Johnston, Phys. Rev. 79, 728 (1950),

6. K. Clusius, A. physik. Chem. B3, 41 (1929).

7. W. F. Giaque and J. O. Clayton, J. Am. Chem. Soc. 55, 4875 (1933).

8. T. A. Scott, J. Chem. Phys. 36, 1459 (1963).

9. A. S. DeReggi, Ph.D. dissertation, University of Florida (1966).

10. V. G. Manzhelii, A. M. Tolkachev, and E. I. Voitovich, Phys. Stat. Sol. St. 13, 351 (1966).

11. P. A. Bezuglyi, L. M. Tarasenko, and Yu. S. Ivanov, Sov. Phys. Sol. St. 10, 1660 (1969).

12. A. Schallamach, Proc. Roy. Soc. (London) A171, 569 (1939).

13. L. Pauling, Phys. Rev. 36, 430 (1930).

14. J. Thomas, N. Alpert, and H. Torrey, J. Chem. Phys. 18, 1511 (1950).

15. A. Crawford, Can. J. Phys. 30, 81 (1952).

16. J. S. Rosenshein, Ph.D. dissertation, Massachusetts Institute of Technology (1963).

17. R. Stevenson, J. Chem. Phys. 27, 656 (1957).

18. J. W. Stewart, J. Phys. Chem. Solids 12, 122 (1959).

19. J. H. Colwell, E. K. Gill, and J. A. Morrison, J. Chem. Phys. 36, 2223 (1962).

20. W. Heuse, Z. physik. Chem. A147, 266 (1936).

21. J. G. Kirkwood, J. Chem. Phys. 8, 205 (1940).

22. T. J. Kreiger and H. M. James, J. Chem. Phys. 22, 796 (1954).

23. B. C. Kohin, J. Chem. Phys. 33, 882 (1960).

24. L. Jansen and F. W. de Wette, Physica 21, 83 (1955).

25. A. S. DeReggi, P. C. Canepa, and T. A. Scott, J. Mag. Resonance 1, 144 (1969).

26. J. C. Raich and R. D. Etters, J. Phys. Chem. Solids 29, 1561 (1968).

27. M. E. Bagatskii, V. A. Kucheryavy, V. G. Manzhelii, and V. A. Popov, Phys. Stat. Sol. 26, 453 (1968).

28. T. A. Keenan and H. M. James, J. Chem. Phys. 31, 12 (1959).

29. T. Yamamoto and Y. Kataoka, J. Chem. Phys. 48, 3199 (1968).

30. R. H. Fowler, Proc. Roy. Soc. (London) A149, 1 (1935).

31. R. H. Fowler, Proc. Roy. Soc. (London) A163, 450 (1937).

32. P. J. Walsh, M. S. Thesis, University of Florida (1963).

33. G. C. Straty, Ph.D. dissertation, University of Florida (1966).

34. M. F. Panczyck, R. A. Scribner, G. C. Straty, and E. D. Adams, Phys. Rev. Letters 19, 1102 (1967).

35. J. W. Philp, Ph.D. dissertation, University of Florida (1969).

36. J. C. Maxwell, A Treatise on Electricity and Magnetism (Dover Publications, Inc., New York) 1, 308 (1954).

37. A. A. Maryott and F. Buckley, Natl. Bur. Standards Cir. 537, 29 (1953).

BIOGRAPHICAL SKETCH

David Craig Heberlein was born in San Antonio, Texas, on January 8, 1942. He attended high school in Arlington, Virginia, graduating from Washington-Lee High School in 1959. After four years at the University of Virginia, he received a B. S. in Physics degree. Since entering the University of Florida in 1963, he has worked as a graduate teaching assistant and as a graduate research assistant.

Mr. Heberlein is married to the former Martha Lois Walkden of Lake Worth, Florida. He is a member of Sigma Pi Sigma.

This dissertation was prepared under the direction of the chairman of the candidate's supervisory committee and has been approved by all members of that committee. It was submitted to the Dean of the College of Arts and Sciences and to the Graduate Council, and was approved as partial fulfillment of the requirements for the degree of Doctor of Philosophy.

August 1969

E. Ruffin Jones
Dean, College of Arts and Sciences

Dean, Graduate School

Supervisory Committee:

E. D. Adams
Chairman

Arthur D. Boyle

James B. Conkling

J. A. Ladd

R. J. Blake